Aalborg University

Master's Thesis

Mathematics-Economics

Analysis of climate- and financial volatility measures and their relation

Mads Bo Andersson

June 3, 2022

AALBORG UNIVERSITET
STUDENTERRAPPORT

Department of Mathematical Sciences
Mathematics-Economics
Skjernvej 4A
DK-9220 Aalborg Ø
http://www.math.aau.dk/

Title

Analysis of climate- and financial volatility measures and their relation

Project Type

Master's Thesis, Mathematics-Economics

Project period

Spring Semester 2022

Author

Mads Bo Andersson

Supervisor

Esben Høg

Page Numbers

61

Appendix pages

51 - 61

Date of Completion

2022-06-03

Abstract

The goal of this thesis is to analyse and construct volatility measures for climate and finance, where the data used to measure the climate is daily temperature anomalies. The global financial market is in this thesis split into the countries of G7 and the countries of BRIC, where the data used is respectively the index S&P 500 and the index MSCI BRIC. Firstly the deterministic seasonality is filtered using a linear model. Secondly the Time-Varying Parameter Vector AutoRegressive model with Stochastic Volatility (TVP-VAR-SV) is used in order to extract the stochastic volatility. Lastly the measures of climate volatility was compared with the measures of financial volatility, where Cross-correlation was used as a comparison measurement.

The results were, that the climate volatility showed *lagged dependency* with the financial volatility measures. The result of this observation was, that the climate volatility was decreasing in the years after a financial volatility spike, thus the climate get improved, when the financial markets worsen. Another result was, that the COVID-19 had a decreasing effect on the climate volatility. Lastly the difference in CO_2 emission of G7 and BRIC did not seem to have an observed effect on the climate volatility.

Further research which could potentially improve the results: Usage of other models like f.x. GARCH and Heston, bigger regions for model construction, improvement on climate change measurement, use more data for construction of financial volatility measure and constructing uncorrelated financial volatility measures.

Preface

This master's thesis is written in the spring of 2022 by Mads Bo Andersson, student in Mathematics-Economics at the Department of Mathematical Sciences, Aalborg University, Aalborg, Denmark.

The document is typeset with LaTeX, data used is downloaded from the data platforms Berkeley Earth [2022], DataHub [2022] and finance [2022], and computations, modelling, and most figures are performed using the *R* language Team [2019] with the packages

- **utils**[1] and **alphaPart**[2] for data import and export.
- **dplyr**[3], **tidyverse**[4] and **lubridate**[5] for data processing.
- **Rcpp**[6], **bvarsv**[7] for modelling.
- **ggplot2**[8] and **ggpubr**[9] for graphical design.

The complete code is not given or described in the text of the document, but it is available upon request.

Reader's Guide:

On page v and page vi, a table of contents is given. When viewing this document as a PDF, hyperlinks in the table of content will allow fast navigation to the desired section.

The bibliography on the pages 47-50 presents the literature used in this document. The source in the bibliography are given in the following format:

[Author][Title](Institution)(ISBN)[Year](URL)(Date Accessed)

Fields in [square brackets] are mandatory, and regular parentheses are only relevant for certain formats (e.g. books or web pages). The bibliography entries are sorted in alphabetical order.

The author would like to acknowledge the project advisor, Esben P. Høg, associate professor, and thank him for his inputs - and his patience - throughout the project period.

[1] Bengtsson [2021]
[2] Gorjanc et al. [2022]
[3] Wickham et al. [2019]
[4] Wickham and RStudio [2021]
[5] Spinu [2021]
[6] Eddelbuettel et al. [2022]
[7] Krueger [2015]
[8] Wickham [2019]
[9] Kassambara [2020]

Contents

Chapter 1

Introduction

Every day, electricity is produced from several different sources globally. This production is divided into fuels made from decomposing plants and animals (coal, oil, gas, etc.) and any hydrocarbon chemical that was not soured from a geological deposit (nuclear, solar, wind, etc.). Fuels are respectively called fossil fuels and non-fossil fuels. The primary energy consumption in the world consist of fossil fuels, which is shown in figure 1.1 on page 1.

The main problem with fossil fuels is, that they are carbon-based and their combustion results in the release of carbon dioxide (CO_2) into the Earth's atmosphere. It is estimated by Explained [2019], that roughly 80% of all man-made CO_2, and the so call *green-house gas* emissions, originate from fossil fuels combustion. These factors traps heat on earth from the sun giving warmer weathers to the globe, resulting in climate change. This will among other things affect various species, cause respiratory and pulmonary diseases and it will contribute to extreme weathers (higher climate volatility).

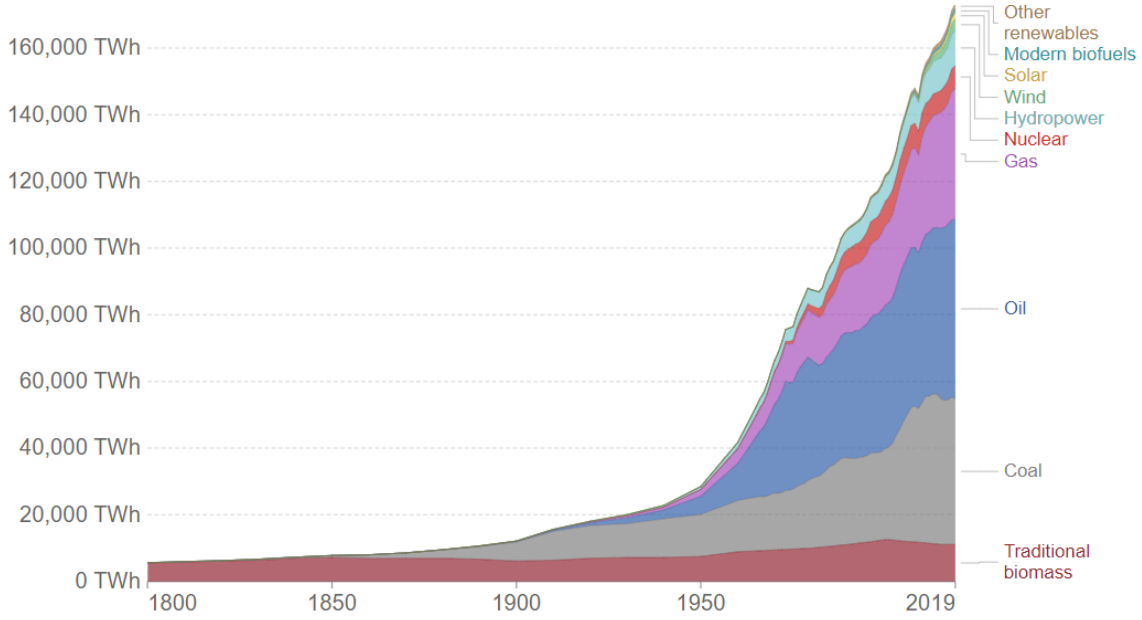

Figure 1.1. Global primary energy consumption by source Smil [2017].

Due to the repercussions of climate changes, scientists around the world have been trying to find solutions to the fossil fuel problems. Given Society [2019] some of the new initiatives is

- New technologies to make commercially available natural-gas-powered vehicles.
- Make coal burning and oil drilling cleaner.
- Usage of more natural gas.
- Remove CO_2 from the atmosphere and store it underground.

These initiatives is only a fraction of the technologies developed on a national scale. Each year, there is discovered more about the consequences of the global warming, and even more

countries join the fight against climate changes. This has lead to an increase in climate research.

1.1 Problem Analysis

With this increasing focus on climate changes and therefore also climate research, one of the main things not investigated is the effect of climate volatility on financial volatility. This result is useful when f.x a government is trying to explain political movement against climate changes, an organization or a corporation is calculating the cost of climate changes and for other applications as well. However it can be a cumbersome job constructing a climate volatility measure and a financial volatility measure. A fair assumption could f.x. be, that the countries of G7[1] is affected differently by climate volatility, than the countries of BRIC[2]. Therefore this project will focus on two financial volatility measures.

Furthermore, if the variables are time dependent, time series analysis is convenient. However studying the time series as univariate time series will not work, since one of the points of interest is how 2 measures affects each other. Therefore a given model should include how 2 (or more) time series affects each other. A way to capture this dependence and use the properties from a multivariate time series is by the use of vector autoregressive models (VAR model), instead of modelling the univariate time series. This project aims furthermore to capture the internal influence of the measures. This leads to the problem statement.

1.1.1 Problem Statement

Based on this summary the focus of the thesis is presented as.

(i) **Analysis of climate- and financial volatility measures**

Which challenges arise, when constructing global volatility measures, and how is it possible to construct the volatility measures using techniques and methods from time series analysis?

(ii) **Dependence structure of these measures**

How can the dependence structure be measured? In recent years the countries of G7 has been focusing on reducing the CO_2 consumption, where the countries CO_2 emissions of BRIC, has been growing at a fast rate for more than a decade. Does this difference in CO_2 emission have an observed effect on the climate volatility measure? How is the volatility of the financial market dependent on the climate volatility?

(iii) **Reaction of these measures to climate disasters**

What is the connection between the climate volatility and the amount of climate disasters? Since the countries CO_2 emissions of BRIC is growing rapidly, this should be depicted in the

[1]The countries of G7 consist of Canada, France, Germany, Italy, Japan, the United Kingdom, the United States and the European Union

[2]The countries of BRIC consist of Brazil, Russia, India and China

climate volatility measure. How does the climate volatility and financial volatility react to this increased CO_2 emission?

1.1.2 Connection with Existing Work

This thesis was originally inspired by the paper of Alessandri and Mumtaz [2021] in which they study the impact of climate volatility on economic growth exploiting data on 133 countries between 1960 and 2005. They use a panel VAR model with stochastic volatility to identify exogenous changes in temperature volatility and assess their implications in macroeconomics. Controlling for temperature levels, a $+1°C$ increase in volatility causes on average a -0.9 percent decline in GDP growth and a $+1.3$ percent increase in the volatility of the GDP growth rate. The work of Alessandri and Mumtaz [2021] inspired several ideas in the author's mind, where some of which are presented here.

1.1.3 Initial data presentation

When constructing climate and financial volatility measures, daily observations can be used, where this thesis will use daily observations of temperature anomalies for the construction of the climate volatility measure. However the financial volatility measure will be divided into two groups: The countries representing G7, and the countries representing BRIC. In order to construct the financial volatility measure of the countries representing G7, daily observations of the S&P 500 index will be used, and to construct the financial volatility measure of the countries representing BRIC, daily observation of the MSCI BRIC index will be used. The three dataset is given below and they will be further elaborated in chapter 4 on page 19.

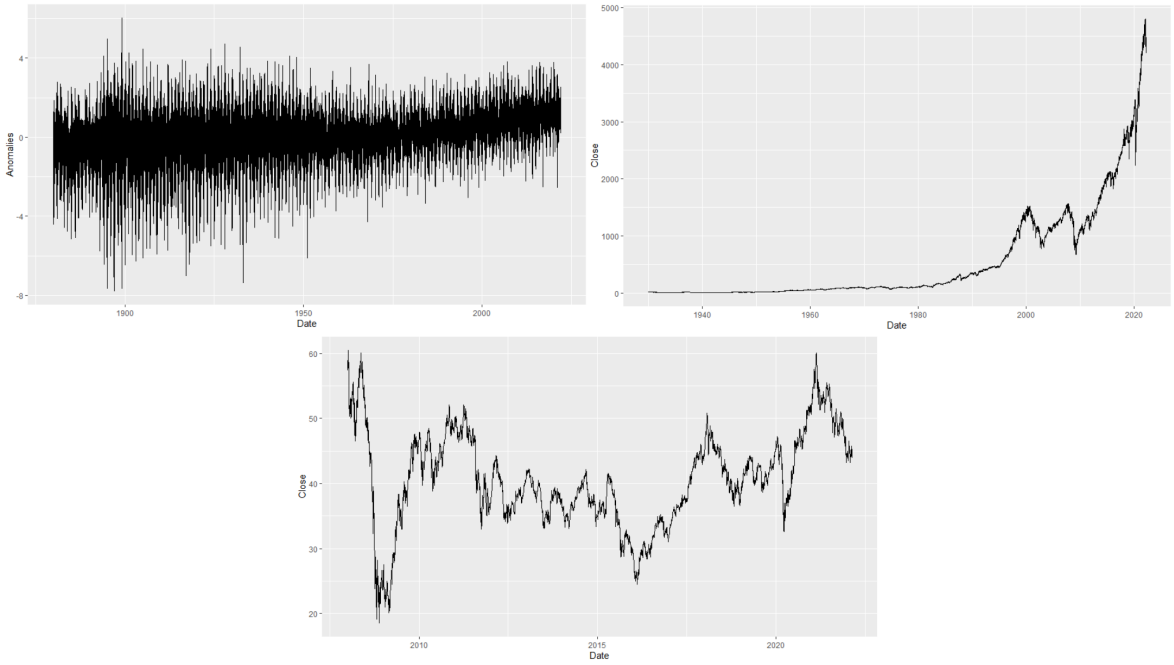

Figure 1.2. The figure on the left is daily observations of temperature anomalies from 1880-2022, the figure on the right is the S&P index from 1930-2022 and the figure at the bottom is the MSCI BRIC index from 2008-2022.

1.2 Thesis Structure

The thesis is split into two parts, where the first part focus on the development of the theoretical foundations and the second part focus on the data analysis. The theoretical part is further subdivided from 2 chapters:

- **Chapter 2** starts by defining the Time-Varying Parameter Vector Autoregressive model with stochastic volatility. Then the Bayesian inference method is introduced, presenting the examples; the inversion method and the rejection method. Lastly the Monte Carlo Markov Chain called the Gibbs sampler is introduced.
- **Chapter 3** is using the theory on multivariate regression in order to explain the Gibbs sampler estimation methodology for the given model. Thus describing the estimations procedure for each parameter.

The second part take the theoretical results and put them to practical use through the joint analysis and modelling of data. This analysis is described in 2 separate chapters:

- **Chapter 4** presents the data and goes into details about which data to use in order to capture the financial market of G7 and BRIC. Furthermore the CO_2 emission for both the countries of G7 and the countries of BRIC is presented. Lastly the data is adjusted to be used in the next chapter.
- **Chapter 5** start by accounting for deterministic seasonality in the dataset. Next it uses the residuals in order to describe the modelling construction, where priors are determined. Then the model is implemented both in a period including the pandemic COVID-19 and before COVID-19. The chapter concludes by measure the Cross-correlation between the volatility measures including and before COVID-19, followed by interpretation of results.

Finally the results and considerations are summarised in **Chapter 6**, where some ideas for further research that arose during the course of the thesis are presented. An list of references is included in the backmatter, along with an appendix.

Chapter 2

Theory on Multivariate Regression

The main object of interest in this thesis is to construct a multivariate time series model with both time varying coefficients and time varying variance matrix of the additive innovations. A drifting component for time variation is used, in order to capture possible nonlinearities or time variation in the lag structure of the model. Furthermore the drifting component for multivariate stochastic volatility is used in order to capture possible heteroskedasticity[1] of the shocks and nonlinearities in the simultaneous relations among the variables of the model. This allows the data to determine whether the time variation of the linear structure derives from changes in impulses (size of the shocks) or response (changes in the propagation mechanism).

There are a few models, which allow for such properties. This thesis will focus on the *Time-Varying Parameter Vector Autoregressive model with Stochastic Volatility* (TVP-VAR-SV) firstly proposed by E. Primiceri [2005], who used it on data for the US monetary policy. This model enables the ability to capture the potential time-varying nature of the underlying structure in the economy in a flexible and robust manner. It has later been used by Nakajima [2011] using Japanese data, which showed a significant structural changes in the dynamic relationship between some macroeconomic variables.

2.1 TVP Vector Autoregressive with Stochastic Volatility

As mentioned before the TVP-VAR-SV model is a multivariate time series model with both time varying coefficients and time varying variance matrix of the additive innovations. The idea of stochastic volatility, which plays an important role in such model, was originally proposed by Black [1976] which followed numerous developments in financial econometrics. Furthermore an application of a model with time-varying coefficients are likely to be inefficient if it assumes constant volatility because of the possibility that the variation of the volatility in disturbances is ignored. Therefore the concept of Stochastic volatility is also incorporated into the empirical analysis.

The model is split into *the Regression*, *the Time-Varying coefficients* and *the Stochastic volatility*. Firstly consider the model

$$y_t = c_t + B_{1,t}y_{t-1} + \cdots + B_{s,t}y_{t-s} + u_t, \qquad t = 1, \cdots, n \tag{2.1}$$

where y_t is an $k \times 1$ vector of observed endogenous[2] variables; c_t is an $k \times 1$ vector of time varying coefficients that multiply constant terms; $B_{i,t}$ for $i = 1, \ldots, s$ are $k \times k$ matrices of time varying coefficients and lastly u_t are heteroskedastic unobservable structural shocks with the variance matrix Ω_t.

It is possible without loss of generality to consider the triangular reduction of Ω_t, which is

[1] If the variability of the random disturbance is different across elements of a given vector of random variables.

[2] It correlates with other factors within the system being studied.

defined by

$$A_t \Omega_t A_t^T = \Sigma_t \Sigma_t^T,$$

where A_t is a $k \times k$ lower triangular matrix and Σ_t is a $k \times k$ diagonal matrix both given as

$$A_t = \begin{bmatrix} 1 & 0 & \cdots & 0 \\ \alpha_{21,t} & 1 & \ddots & \vdots \\ \vdots & \ddots & \ddots & 0 \\ \alpha_{k1,t} & \cdots & \alpha_{kk-1,t} & 1 \end{bmatrix}, \quad \Sigma_t = \begin{bmatrix} \sigma_{1,t} & 0 & \cdots & 0 \\ 0 & \sigma_{2,t} & \ddots & \vdots \\ \vdots & \ddots & \ddots & 0 \\ 0 & \cdots & 0 & \sigma_{k,t} \end{bmatrix},$$

where $\alpha_{ij,t}$ is time varying components and $\sigma_{i,t}$ is the standard deviation for $i, j = 1, \ldots, k$.

Using the triangular of Ω_t, the equation 2.1 on page 5 can be written as

$$y_t = c_t + B_{1,t} y_{t-1} + \cdots + B_{s,t} y_{t-s} + A_t^{-1} \Sigma_t \epsilon_t, \tag{2.2}$$

$$Var(\epsilon_t) = I_k. \tag{2.3}$$

By stacking all of the B_t in a single $(k^2 s \times 1)$ vector, then the **Regression** model can be written by using equation 2.2 as

$$y_t = \mathbb{X}_t^T B_t + A_t^{-1} \Sigma_t \epsilon_t, \tag{2.4}$$

$$\mathbb{X}_t^T = I_k \otimes [1, y_{t-1}^T, \ldots, y_{t-s}^T], \tag{2.5}$$

where $\otimes$ denotes the Kronecker product (see definition 2 on page 51).

It is worth noticing that it is crucial for a TVP-VAR-SV model that the matrix A_t should be time varying. Otherwise it would imply that an innovation to the ith variable has a time invariant effect on the jth variable. Since the objective is modelling time variation in a simultaneous equation model, where simultaneous interactions among the variables are fundamental, the modelling strategy consist of modelling the coefficient processes in equation 2.4.

Now let $\alpha_t = (\alpha_{21,t}, \alpha_{31,t}, \alpha_{32,t}, \ldots, \alpha_{kk-1,t})^T$ be the vector of the non-zero and non-one elements of the matrix A_t stacked by rows. Furthermore let $h_t = (h_{1,t}, \ldots, h_{k,t})^T$ be the measurement of stochastic volatility such that $h_{j,t} = log(\sigma_{j,t})$, for $j = 1, \ldots, k$. Then the dynamics of the model's **Time-Varying** parameters is specified as

$$B_t = B_{t-1} + v_t, \tag{2.6}$$

$$\alpha_t = \alpha_{t-1} + \zeta_t, \tag{2.7}$$

$$h_t = h_{t-1} + \eta_t, \tag{2.8}$$

where the elements of the vector B_t, α_t and h_t are modeled as random walks. Furthermore is the standard deviations (σ_t) assumed to evolve as geometric random walks[3], which belongs to the model class **Stochastic Volatility**. The variances generated by equation 2.8 are then unobservable components, which is an important observation in the estimation process described later.

[3] see Vempala [2005]

The innovations in the model are all assumed to be jointly normally distributed with a mean value of 0 and the following assumptions on the variance matrix

$$V = Var\left(\begin{bmatrix}\epsilon_t\\ v_t\\ \zeta_t\\ \eta_t\end{bmatrix}\right) = \begin{bmatrix}I_k & 0 & 0 & 0\\ 0 & Q & 0 & 0\\ 0 & 0 & S & 0\\ 0 & 0 & 0 & W\end{bmatrix}, \tag{2.9}$$

where Q, S and W are positive definite matrices. It is worth noticing, that all the zero blocks could be substituted by non-zero blocks with only some small modifications on the estimation procedure. However there are at least two reasons not to. **Firstly** it would lead to too many parameters of the model. This would require the specification of a sensible prior, to be able to prevent the cases of ill-determined parameters. The **second** reason is, that it preclude any structural interpretation of the innovations, when allowing for a completely generic correlation structure among different sources of uncertainties.

When working with time series analysis it is an undesirable implication to include random walk processes, since they hit any upper or lower bound with the probability of one. However since the equations 2.6, 2.7 and 2.8 are thought to be in place for a finite period of time, those usually assumptions should be innocuous. Furthermore an advantages of the random walk assumption is, that it focus on permanent shifts and reduces the number of parameters in the estimation procedure.

Now that the TVP-VAR-SV model is presented, the objective is to lay out some of the econometric techniques used to estimate the model. The stochastic volatility makes the estimation process difficult because the likelihood function becomes intractable, since as mentioned before the variances generated by equation 2.8 on page 6 are unobservable components. However it is possible to estimate the model using *Markov Chain Monte Carlo* (MCMC) methods in the context of a Bayesian inference. Firstly the Bayensian inference will be elaborated upon, and thus the MCMC will be further elaborated in section 2.3.2 on page 13.

2.2 Bayesian Inference

Wasserman [2010,p. 175-178] explains, that there are two main approaches to statistical machine learning: The frequentist methods and the bayesian methods. Those point of views is based on the following postulates:

Frequentist point of view	Bayesian point of view
Probability refers to limiting relative frequencies, and the probabilities are therefore objective properties of the real world.	Probability describes degree of belief, and not the limiting frequency.
Parameters are fixed, unknown constants. Since they do not fluctuate, it is not possible to make useful probability statements about the parameters.	It is possible to make probability statements about parameters even though they are fixed constants
Statistical procedures should be designed to have well-defined long run frequency properties, such that f.x. a 95% confidence interval traps the true value of the parameter with limiting frequency at least 95%.	Inferences about a parameter is made by producing a probability distribution of the parameter, and then extracting the inferences (such as point estimates and interval estimates) from the distribution.

Table 2.1. The Frequentist and Bayesian point of view

This thesis will be focusing on the Bayesian inference. The Bayesian inference method is usually carried out using the following procedure

- Firstly without the use of data a probability density function $f(\theta)$ expressing a belief about a parameter θ is chosen. This is also called the **prior distribution**.
- Secondly a statistical model $f(x \mid \theta)$ reflecting the belief is chosen.
- Lastly using given n observations $X_1, \ldots, X_n$, the beliefs is updated, and the **posterior** distribution $f(\theta \mid X_1, \ldots, X_n)$ is calculated.

To further elaborate upon the last step firstly assume that there exist n i.i.d. observations $x_1, \ldots, x_n$, such that the likelihood can be written as

$$f(x_1, \ldots, x_n \mid \theta) = \prod_{i=1}^{n} f(x_i \mid \theta) = \mathcal{L}_n(\theta).$$

Now the Bayes' theorem[4] can be used in order to write the continuous posterior distribution as

$$\begin{aligned} f(\theta \mid x_1, \ldots, x_n) &= \frac{f(x_1, \ldots, x_n \mid \theta) f(\theta)}{\int f(x_1, \ldots, x_n \mid \theta) f(\theta) d\theta}, \\ &= \frac{\mathcal{L}_n(\theta) f(\theta)}{b_n} \propto \mathcal{L}_n(\theta) f(\theta), \end{aligned}$$

where

$$b_n = \int \mathcal{L}_n(\theta) f(\theta) d\theta,$$

[4]See Lynch [2007,p. 47-51].

is called the **normalizing constant**, which is not dependent on θ. Thus b_n doesn't affect the maximization or minimization process of θ, and it can be recovered later, if needed to.

Now that the posterior distribution is obtained, the point estimate can be obtained by summarizing the center of the posterior. Typically it suffice to use the mean of the posterior, which is

$$\bar{\theta}_n = \int \theta f(\theta \mid x_1, \ldots, x_n) d\theta = \frac{\int \theta \mathcal{L}_n(\theta) f(\theta)}{\int \mathcal{L}_n(\theta) f(\theta) d\theta}.$$

Furthermore the Bayesian interval estimate can be calculated. In order to do this, let a and b be constants, such that $\int_{-\infty}^{a} f(\theta \mid x_1, \ldots, x_n) d\theta = \int_{b}^{\infty} f(\theta \mid x_1, \ldots, x_n) d\theta = \alpha/2$. Furthermore let $C = (a, b)$ be the open interval between a and b. Then

$$\int_a^b f(\theta \mid x_1, \ldots, x_n) d\theta = 1 - \alpha,$$

where C is called a $1-\alpha$ posterior interval. To continue the explanation on Bayesian inference, a some notation framework needs to be defined.

> In order to denote the history of a generic vector of variables $\varkappa_t$ up to a generic time τ, the following notation is used:
>
> $$\varkappa^\tau = [\varkappa_1^T, \ldots, \varkappa_\tau^T]^T.$$
>
> Furthermore in order to denote the history of a generic matrix of variables and constant terms M_t up to a generic time τ, the following notation is used:
>
> $$M^\tau = [m_1^T, \ldots, m_\tau^T]^T,$$
>
> where m_t is a column vector constructed with the time varying elements of M_t.

As stated before the Bayesian methods is used in order to evaluate the posterior distributions of the parameters of interest. In the case of the TVP-VAR-SV model, this is the unobservable states B^n, A^n, Σ^n and the hyperparameters of the variance matrix V. There are four reasons why the Bayesian methods is particularly suitable in the estimation of this class of models and why it is preferred over classical estimation, which often involve the use of standard likelihood functions.

Firstly the estimation process must be able to handle unobservable components. **Secondly** Stephard and Harvey [1989] explains, that if the variance of the time varying coefficients is too small, the classical maximum likelihood estimator would behave in an unusual way. A **third** drawback of using the classical maximum likelihood is the high dimensionality of the TVP-VAR-SV model and the non-linearity. Therefore the possibility arises, that the likelihood of such model would have multiple peaks and that these peaks could be very narrow leading to the possibility of the likelihood reaching very high values, which would not be representative of the model's fit on a wider parameter region. Here the Bayesian approach use an uninformative priors on reasonable regions of the parameter space, which can effectively prevent this from happening.

The **fourth** and the last reason is, that it is a cumbersome job to maximize the likelihood over a high dimensional space. Here Bayesian methods splits the original estimation problem into smaller and simpler ones. To do this different sampling methods can be used.

For some distributions the integrals for summarizing the posterior distributions can be easily computed using numerical methods or they have closed-form solutions and are known. However for many distributions this is not the case, and the integrals may not be easy to compute. Usually the Bayesians would remedy this problem by working with conjugate priors[5]. The conjugate priors can however sometimes be unrealistic, or the model may involve distributions, which are not suited for simple computation of quantiles and other quantities. In those cases, two basic approaches are used to compute integrals:

- Approximation methods.
- Sampling methods.

The approximations methods is commonly used, when the true function is unknown, and only a rough idea of the main properties are needed. The methods can also be used, when it is too costly either in terms of time or complexity to compute the true function. This could f.x. involve the use of quadrature methods, Taylor series expansions and mixture of normals. However Lynch [2007,p. 77-105] states, that it can be beneficial not to rely on the asymptotic arguments used in approximations methods. As a result this thesis will not focus on those methods [6].

As mentioned before sampling methods constitute an alternative to approximation methods. Lynch [2007,p. 77-105] states, that the general idea of the sampling approach is to make it possible to estimate f.x. the mean and variance by generating a sample of size n from the distribution of interest,

$$\int \theta f(\theta \mid x^n) d\theta \approx \frac{1}{n}\sum_{i=1}^{n} \theta_i = \mu_\theta,$$

$$\int (\theta - \mu_\theta)^2 f(\theta \mid x^n) d\theta \approx \frac{1}{n}\sum_{i=1}^{n} (\theta_i - \mu_\theta)^2 = \sigma_\theta^2.$$

For many distributions, there exists effective routines for simulation. However for other distributions, an extant routine should be specified. Here Lynch [2007,p. 77-105] present two basic sampling methods namely the *inversion method* and the *rejection method*.

2.2.1 Inversion method of sampling

In this section it should be noted, that the cumulative distribution function $F(\cdot)$ of the probability density function $f(\cdot)$ is monotone increasing. An additional assumption of this method is that the inverse cumulative distribution function $F^{-1}(\cdot)$ exist and that it can be derived analytically. The inversion method is used to draw a sample from a univariate distribution[7] $f(x)$ using the following two step procedure.

1. Draw a uniform random number, $u \sim U(0, 1)$.
2. Let $z = F^{-1}(u)$ be the draw from $f(x)$.

The inversion method is efficient and easy to implement. However if it is impossible to derive the inverse function analytically, then this method cannot be used. Furthermore the inversion

[5] If the posterior distribution is same probability distribution family as the prior probability distribution.
[6] See Judd [1998,p. 195-247] for further elaboration on approximation methods
[7] see Levy [2012,p. 14-15] for more information

method does not work on multivariate distributions, since the inverse is generally not unique beyond one dimension. This motivates the use of the rejection method of sampling.

2.2.2 The rejection method of sampling

As mentioned the rejection method of sampling is motivated due to the drawbacks of the inversion method. Here it is assumed that $F^{-1}(u)$ cannot be computed analytically. Let $U(a, b)$ denote the uniform cumulative distribution[8]. Then the rejection sampling samples from a distribution $f(x)$ for x, and it uses the following four step procedure.

1. Generate z from a distribution $g(x)$ from which sampling is easy and then scale $g(x)$ by the constant m, such that $m \cdot g(x)$ is greater than $f(x)$.
2. Compute $R = \dfrac{f(z)}{m \cdot g(z)}$.
3. Sample $u \sim U(0, 1)$
4. If $R > u$, then accept z as a draw from $f(x)$. Otherwise, repeat from step 1.

The increment $m \cdot g(x)$ is called an *envelope function*, due to the requirement from step one.

This method can be used to sample from any density, meaning that it is also possible to sample from multivariate densities. However in the multivariate case a random vector is chosen, rather than a single point.

The rejection sampling method does however have some limitations. **Firstly** finding the (enveloping) function $m \cdot g(x)$ with values greater at all points of support for the density of interest may be a cumbersome task. **Secondly** if the enveloping function is considerably higher than $f(x)$ at all points (f.x. if m is huge), the algorithm would reject most attempted draws. This could lead to the algorithm being very inefficient. Since the dimensionality increases in multivariate distributions, the rejection sampling would still be possible, but it would be increasingly difficult as the dimensions of the model increases.

[8] see Levy [2012,p. 14-15] for more information

2.3 Bayesian Numerical Computation

The disadvantages of the previously methods of sampling motivates the need for other methods. This section is used to lay the foundation for the numerical computation framework of such methods.

2.3.1 Monte Carlo Integration

As mentioned before the Bayesian Inference output is the posterior distribution and one is often interested in estimating the posterior mean. If analytical expression are readily available, Rachev et al. [2008,p. 61-77] suggest, that the integral defining the posterior mean can be computed analytically. Denoting the unknown parameter vector by θ and the observed data as y, the conditional posterior mean of a function $g(\theta)$ is given by

$$\mathbb{E}[g(\theta) \mid y] = \int g(\theta) f(\theta \mid y) d\theta,$$

where the posterior distribution of θ is given as $f(\theta \mid y)$.

Now the Monte Carlo can be used. The Monte Carlo technique is a numerical method for randomly sampling a probability distribution and approximating a desired quantity for which an analytical solution is not known. It is constructed by computing an approximation using the *Strong Law of Large Numbers*[9]. Suppose it is possible to obtain a independent sample $\theta^{(1)}, \ldots, \theta^{(r)}$ from the posterior distribution. Then Rachev et al. [2008,p. 61-77] states, that the quantity

$$\widehat{g_r(\theta)} = \frac{1}{r} \sum_{i=1}^{r} g(\theta^{(i)}),$$

converge to $\mathbb{E}[g(\theta) \mid y]$ as r goes to infinity. This approximation procedure is called the *Monte Carlo integration*, and will be referred to as the Monte Carlo approximation.

It is possible to use the asymptotic variance of $\widehat{g_r(\theta)}$ to evaluate the quality of the approximation. This means, that it is possible to evaluate the variance of $g(\theta)$ using the sample variance,

$$s_r^2 = \sqrt{\frac{1}{r} \sum_{i=1}^{r} \left(g(\theta^{(i)}) - \widehat{g_r(\theta)})^2 \right)}.$$

Thus it is possible to measure the numerical accuracy using

$$MCSE = \sqrt{\frac{s_r^2}{r}},$$

which is called the *Monte Carlo Standard Error* (MCSE).

[9] See Sedor [2015] for further elaborating.

2.3.2 Monte Carlo Markov Chain

It is not always possible to simulated i.i.d. draws from a complicated posterior density. Thus in order to avoiding the independence assumption, the posterior simulation algorithms, known as Monte Carlo Markov Chain methods, provide iterative procedure to approximately sample from posterior densities. At each step, the algorithm tries to find parameter values with higher posterior probability. Thus the approximation will move closer to the target posterior density. The MCMC methods is expanded such that the simulations of θ are obtained as the realizations of *Markov chains*.

Definition 1: Markov Chain

A sequence $X_1, \ldots, X_n$ of random variables in discrete time is called a *Markov chain* if any state of the process is only dependent on the previous state, and not on any earlier state. This can be written as

$$\mathbb{P}(X_n = x \mid X_1 = x_1, \ldots, X_{n-1} = x_{n-1}) = \mathbb{P}(X_n = x \mid X_{n-1} = x_{n-1}).$$

A Markov chain has to satisfy a number of properties (such as irreducibility and ergodicity) in order to be able to converge to its so called *stationary distribution*. Generally those properties result in, that the chain can reach any state from any other state in a finite number of steps (See Robert and Casella [2010,p. 61-69] and Sharma [2017,p. 16-20] for rigorous definitions of the properties of Markov chains).

The two most commonly employed MCMC is the *Metropolis-Hastings* algorithm[10] and the *Gibbs Sampler*. This thesis will focus on the Gibbs sampler.

2.3.3 Gibbs sampling

The Gibbs sampler was first introduced by Geman and Geman [1984,p. 721-741], and it is a special case of the more general Metropolis-Hastings algorithm. It is used to construct the posterior numerical evaluation of the parameters of interest. The Gibbs sampler constructs a Markov chain whose values converge towards a target distribution, and it is used when the joint distributions is not known explicitly but the conditional distribution of each variable is known and is easy to sample from. Furthermore it is a particular variant of MCMC methods, which draws an instance from lower dimensional conditional posterior, to prevent the high dimensionality of the joint posterior of the whole parameter set. Let $\theta_1, \ldots, \theta_r$ be parameters of interest. Then the Gibbs samplers procedure is the following iterative process.

[10] See Metropolis et al. [1953] for further information.

Algorithm 1 The Gibbs sampling

1. Assign a vector of starting values to the parameter vector, $\Theta^{j=0}$.
2. Set $j = j + 1$.
3. Sample $(\theta_1^j \mid \theta_2^{j-1}, \theta_3^{j-1}, \ldots, \theta_r^{j-1})$.
4. Sample $(\theta_2^j \mid \theta_1^j, \theta_3^{j-1}, \ldots, \theta_r^{j-1})$.
5. $\vdots$
6. Sample $(\theta_r^j \mid \theta_1^j, \ldots, \theta_{r-1}^j)$.
7. Repeat step 2 until convergence is achieved.

Here j is an index for the iteration count. In that sense the Gibbs sampler keeps updating the parameters each iteration.

Special for the Gibbs sampling is, that the full conditional density for a parameter needs only to be known up to a normalizing constant[11]. Thus it is possible to continue the parameter calculation, and then using the joint density. Once all other parameters are treated as fixed, the Gibbs sampling is therefore relatively simple for most problems, where the joint density can be reduced to known forms for each parameters.

The MCMC is a smoothing method. It estimates the parameters of interest based on the entire available set of data. As opposed to filtered estimates, smoothed estimates depends on the specific problem at hand, and they can not be established as knowledge, which proceeds from theoretical deduction. When the objective is an investigation of the true evolution of the unobservable states over time, smoothed estimates are more efficient. In those cases, it would be inappropriate to use filtered estimates, since they would exhibit short-term variation even in time invariant models. Filtered estimates would therefore be more appropriate if the objective of the investigation is constructing model diagnostics or forecasting evaluation.

[11] See J. Keffer [2015,p. 26-46] for further details.

Chapter 3

Estimation Methodology

This chapter is designed for the estimation procedure of the TVP-VAR-SV model illustrated in chapter 2 on page 5. This chapter will be based on E. Primiceri [2005].

3.1 Estimation Procedure

The estimation procedure for the TVP-VAR-SV model is done using the Gibbs sampler algorithm 1 described on page 14. Let $y = \{y_i\}_{i=1}^n$, $B = \{B_i\}_{i=1}^n$, $\alpha = \{\alpha_i\}_{i=1}^n$, $h = \{h_i\}_{i=1}^n$ and $\omega = (Q, S, W)$. Then set the prior probability density as $f(\omega)$ for ω. Now given the data y, then it is possible to draw samples from the posterior distribution, $f(B, \alpha, h, \omega \mid y)$ using the following algorithm.

Algorithm 2 TVP-VAR-SV estimation algorithm

1. Assign initial values for B, α, h and ω.
2. Sample $(B \mid \alpha, h, Q, y)$.
3. Sample $(Q \mid B)$.
4. Sample $(\alpha \mid B, h, S, y)$.
5. Sample $(S \mid \alpha)$.
6. Sample $(h \mid B, \alpha, W, y)$.
7. Sample $(W \mid h)$.
8. Return to step 2

The specific details of the procedure is illustrated as follows.

3.1.1 Sample B

Firstly the objective is to sample B from the conditional posterior distribution. This is done by constructing a state space model with respect to B_t as the state variable which is written as

$$\begin{aligned} y_t &= X_t B_t + A_t^{-1}\Sigma_t \epsilon_t, & t &= 1, \ldots, n, \\ B_{t+1} &= B_t + \nu_t, & t &= 0, \ldots, n-1, \end{aligned}$$

where $B_s = \nu_0$ and $\nu_s \sim (0, Q)$. Now the simulation smoother can be used, which is given in appendix A.1.4 on page 53, where the variables is substituted by

$$\begin{aligned} X_t\beta &= 0, & Z_t &= X_t, & G_t &= (A_t^{-1}\Sigma_t, 0) \\ T_t &= I_{k_\beta}, & H_t &= (0, Q^{1/2}), \end{aligned}$$

where k_β is the number of rows β.

3.1.2 Sample α

The system of equation given in equation 2.4 on page 6 can be written as

$$\begin{aligned} y_t - X_t^T B_t &= A_t^{-1}\Sigma_t\epsilon_t \\ A_t \underbrace{(y_t - X_t^T B_t)}_{:=\hat{y}_t} &= \Sigma_t\epsilon_t. \end{aligned} \tag{3.1}$$

Here B_t is given from section 3.1.1 and $\hat{y}_t$ is observable. Since A_t is a lower triangular matrix with ones in the diagonal, it can be split into two matrixes; a matrix $K^{(1)}$ with the α_t in the lower off-diagonal and the identity matrix I_{n^2}. Then using this property, it is possible to rewrite equation 3.1 as

$$\hat{y}_t = \Sigma_t\epsilon_t - K^{(1)}\hat{y}_t.$$

Now multiplying $\hat{y}_t$ on $K^{(1)}$ and draw α_t out of K, thus constructing the matrix $K^{(2)}$, results in

$$\hat{y} = \Sigma_t\epsilon_t - K^{(2)}\alpha_t, \tag{3.2}$$

where α_t is defined as in equation 2.7 on page 6. Next by changing the signs of the inside of $K^{(2)}$, creates the matrix Z_t, which is the following $k \times \dfrac{k(k-1)}{2}$ matrix:

$$Z_t = \begin{bmatrix} 0 & \cdots & \cdots & 0 \\ -\widehat{y}_{1,t} & 0 & \cdots & 0 \\ 0 & -\widehat{y}_{[1,2],t} & \ddots & \vdots \\ \vdots & \ddots & \ddots & 0 \\ 0 & \cdots & 0 & -\widehat{y}_{[1,\ldots,k-1],t} \end{bmatrix},$$

where the $\widehat{y_{[1,\ldots,i],t}}$ denotes the row vector $[\widehat{y_{1,t}} \ \ldots \ \widehat{y}_{i,t}]$ for $i = 1, \ldots, (k-1)$. Thus it is possible to rewrite equation 3.2 on page 16 as

$$\hat{y}_t = Z_t\alpha_t + \Sigma_t\epsilon_t.$$

Now in order to sample α_t, the simulation smoother can be run with the correspondences:

$$\begin{aligned} X_t\beta &= 0, & Z_t &= Z_t, & G_t &= (\Sigma_t, 0) \\ T_t &= I_{k_\alpha}, & H_t &= (0, S^{1/2}), \end{aligned}$$

where k_α is the number of rows of α_t.

3.1.3 Sample h

As before consider the system of equations

$$A_t(y_t - X_t^T B_t) = \Sigma_t \epsilon_t = y_t^*,$$

where this system is constructed such that both B^n and A^n is given from respectively section 3.1.1 and section 3.1.2, and y_t^* is observable. This system consist of nonlinear measurement equations[1]. Therefore squaring and taking logarithms of every element can convert the system into a system of linear measurement equations. Thus defining $y_{i,t}^{**} = log\left((y_{i,t}^*)^2 + c^{off}\right)$, where c^{off} is an offset constant (often set equal to 0.001). The offset constant is used in order to make the estimation procedure more robust, since $y_{i,t}^2$ can be very small. This result in the following approximating state space representation:

$$\begin{aligned} y_t^{**} &\approx 2h_t + e_t \\ h_t &= h_{t-1} + \eta_t, \end{aligned}$$

where $e_{i,t} = log(\epsilon_{i,t}^2)$. Notice that e_t and η_t are not correlated.

The innovations in the measurement equations are distributed as a $log(\chi^2(1))$. Therefore the system has a linear, but non-Gaussian state space form. To transform the system into a Gaussian one, a mixture of normal approximation of the $log(\chi^2(1))$ distribution is used, which is explained by Kim et al. [1998,p. 370-374]. Furthermore since the variance matrix of ϵ's is the identity matrix, the variance matrix of the e's would also be diagonal.

Using the previous notations, let $b^n = [b_1 \ldots, b_n]^T$ be defined as the matrix of indicator variables selecting where the member of mixture of normal approximation has to be used for each element of e, at every point in time. Thus conditional on B^n, A^n, V and b^n, where V is defined in equation 2.9 on page 7, it is possible to use the approximate linear and Gaussian state space form of the system. This would open up for the procedure, which recursively recover

$$\begin{aligned} h_{t|t+1} &= \mathbb{E}\left[h_t \mid h_{t+1}, y^t, A^n, B^n, V, b^n\right], \\ H_{t|t+1} &= Var\left(h_t \mid h_{t+1}, y^t, A^n, B^n, V, b^n\right). \end{aligned}$$

The objective is to recursively draw every $h_{t|t+1}$ from the generic density function $f(h_t \mid h_{t+1}, y^t, A^n, B^n, V, b^n)$, which is $\mathcal{N}(h_{t|t+1}, H_{t|t+1})$ distributed. Then it is possible calculate the entirety of $h_{t|t+1}$ using the simulation smoother given in appendix A.1.4 on page 53. For the selection of mixtures Kim et al. [1998,p. 370-374] suggest using a mixture of 7 normal densities. Then the sampling of the b^n matrix conditioned on $(y^{**})^n$ and h^n can be done by independently sample each of the $b_{i,t}$ using the probability mass function

$$\mathbb{P}\left(b_{i,t} = j \mid y_{i,t}^{**}, h_{i,t}\right) \propto q_j f_{\mathcal{N}}\left(y_{i,t}^{**} \mid 2h_{i,t} + o_j - 1.2704, v_j^2\right),$$

where $j = 1, \ldots 7$ and $i = 1, \ldots, n$. Here $f_{\mathcal{N}}$ represents the normal density with the component probabilities q_j. The mean of the model is given as $o_j - 1.2704$ and the variances is given as v_j^2. The constants $\{q_j, o_j, v_j^2\}$ are selected in order to closely approximate the exact density, i.e. they are chosen to match a number of moments of the $log(\chi^2(1))$ distribution.

[1] Fx. $y_{i,t}^* = \exp(h_{i,t})\epsilon_{i,t}$.

3.1.4 Sample hyperparameters

Lastly the objective is to sample the hyperparameters. The hyperparameters of the model are the diagonal matrices of V, i.e. Q, W and the diagonal block matrices of S, since I_n is given[2]. Therefore conditioned on B^n, Σ^n, A^n and y^n, an independent inverse-Wishart posterior distribution[3] can be made for each square block, and since the innovations are observable, it is easy to draw from these inverse-Wishart posteriors[4]. Thus it is possible to sample V, by sampling Q, W and S from

$$\begin{aligned} f(Q, W, S \mid y^n, B^n, A^n, \Sigma^n) = & f(Q \mid y^n, B^n, A^n, \Sigma^n) f(W \mid y^n, B^n, A^n, \Sigma^n) \cdots \\ & f(S_1 \mid y^n, B^n, A^n, \Sigma^n) \cdots f(S_{k-1} \mid y^n, B^n, A^n, \Sigma^n)). \end{aligned}$$

Now given data, it is possible to estimate a model by simulating the distribution of the parameters of interest. Here Gibbs sampling is used to exploit the blocking structure of the unobservable parameters. The procedure is to in-turn draw;

1. The time-varying coefficients (B^n),
2. The simultaneous relations (A^n),
3. The volatility (h^n),
4. Lastly the hyperparameters (V),

conditional on the observed data and the parameters.

[2]This is corresponding to the parameters belonging to different equations.
[3]See W. Nydick [2012,p. 1-12].
[4]The sampling procedure is described by Hoijtink [2008,p. 6-12].

Chapter 4

Data Analysis

This chapter is designed for the construction and analysis of data representing climate and the financial market, which later will be used in constructing the volatility measures.

Climate Volatility can be defined as the degree of changeability or variance in ambient climatic conditions over time. A measurement for Climate Volatility can be constructed using many different methods and data. One of the intuitions is, that it should be constructed using data from weather. Such data is measured by weather stations all over the globe, which measures the temperature, atmospheric pressure, humidity, wind speed, etc. As mentioned before the data used in this thesis is the daily land-surface average anomaly results from Berkeley Earth [2022] produced by the averaging method. The data is given in the period starting in 1880-01-01 and ending on 2021-12-31. Berkeley Earth is an independent U.S. non-profit organization focused on environmental data science. They supply comprehensive open-source world air pollution data and highly user-accessible global temperature data that is timely, impartial, and verified. Daily observations of temperature anomalies is once more presented below

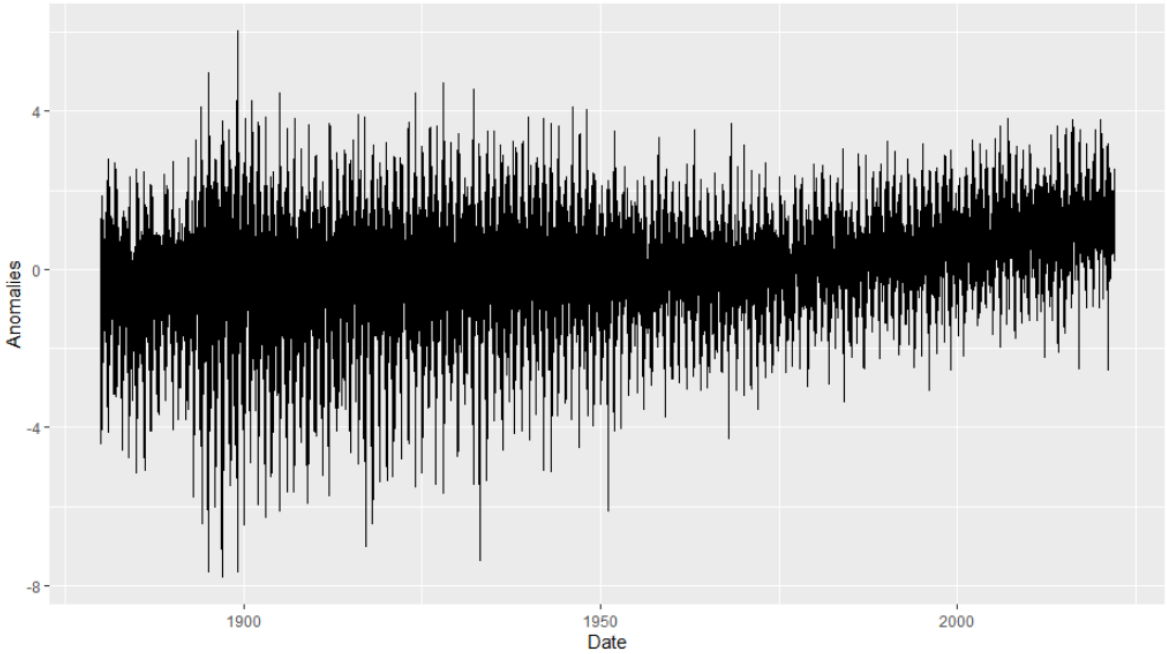

Figure 4.1. Daily observations of temperature anomalies from 1880-2022.

The temperatures are displayed in Celsius degrees, and they are reported as anomalies. One occurring problem, when measuring climate changes is, that the temperature between countries tend to vary differently from each other. However a reasonable assumption is, that even though the actual temperatures is different in each area, the temperature deviation is the same. Therefore in order to measure climate change, temperatures anomalies are often used. A temperature anomaly is defined as the difference between the measured temperature and a reference baseline temperature, which in this case is defined as the average temperature in the period 1951-1980.

Temperature anomalies are used due to the fact that temperatures is location variant, where f.x. the polar region is colder than the tropics and the atmospheres temperature varies across atmosphere layers. Thus the advantages of using anomalies is, that they are constant over large areas, meaning if it is a degree warmer in the polar region, chances are that it is a degree warmer in the tropics.

4.1 Financial data analysis

Where it was possible to use only data of temperatures anomalies when measuring climate change, this is not the case when measuring the financial market across the globe. This is due to, that no dataset covers the entirety of the global financial market, f.x. the financial market of Denmark, China, USA and South Africa at the same time. However the countries of the G7 and the countries of BRIC both covers a big chunk of the global economy.

The G7 (also called the group of seven) is an inter-governmental political forum with origin in 1973 consisting of Canada, France, Germany, Italy, Japan, the United Kingdom and the United States. The G7 expanded later into the G20, which included 12 more countries and the European Union. However since the BRIC countries is a member of G20, this thesis focus on the G7 countries.

The BRIC index originally dates from 2001 and refers to the countries Brazil, Russia, India and China. They are among the largest countries in the world, and it is stated by Haugaard and Larsen [2004,p. 39-51], that the BRIC countries also dominate the emerging market economies[1]. The grouping acronym was originally projected with the mindset, that the BRIC nations would grow quickly, their economies would eventually be larger of those of the G7 and, as Mostafa and Mahmood [2015,p. 156-170] states, they would dominate the world economy by 2040.

[1] An emerging market economy is the economy of a developing nation that is becoming more engaged with global markets as it grows.

4.2 Climate changes of G7 and BRIC

Together, the G7 and the BRIC countries make up a large part of the global economy. As a result, they contribute to the global energy production, thus contributing to the global carbon dioxide (CO_2) emission. In fact in 2020 the countries of the G7 and BRIC were respectively responsible for 22.5% and 43.54% of the worlds CO_2 emission. It is stated by Wu et al. [2021], that increased concentration of CO_2 in the atmosphere have impacted climate changes resulted in the concept global warming. The CO_2 emission from the countries of G7 and BRIC in the period $1950 - 2020$ are respectively shown in the following figures.

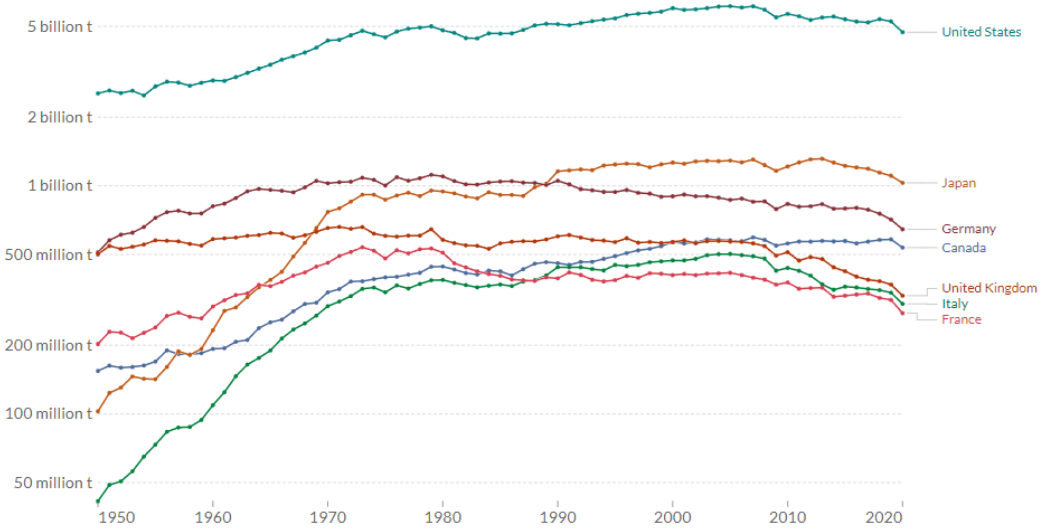

(a) The CO_2 emission from the countries of G7.

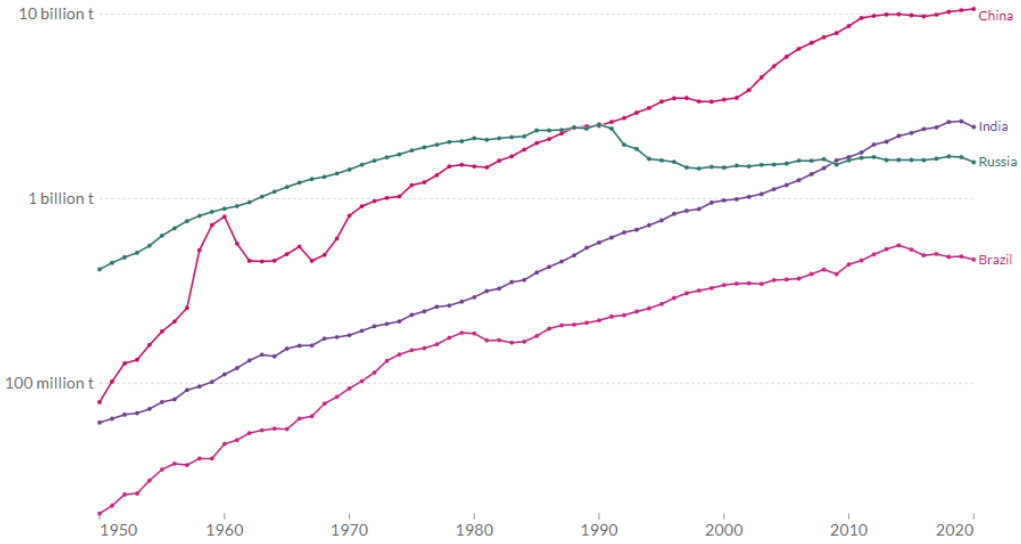

(b) The CO_2 emission from the countries of BRIC.

Figure 4.2. CO_2 emissions from the burning of fossil fuels for energy and cement production. Land-use change is not included (Source: Hannah Ritchie and Rosado [2020]).

The *land-use change* is the CO_2 emission caused from a modification a country does to the natural landscape. In the above figures it can be seen, that from 1950 to 2020 there has been an acceleration of CO_2 production both in the countries of G7 and BRIC. However where the CO_2 emission from the countries of G7 looks almost stable from 1980 and forward, the CO_2 emission from the countries of BRIC looks to be accelerating throughout the whole period. This is most clearly seen observing the CO_2 emission from China, which went from 1 billion ton in 1973 to 10 billion ton in 2012.

As stated before this acceleration of CO_2 in the atmosphere have impacted climate changes. The human-induced climate change causes among other things more frequent and intense extreme weather events, and furthermore increases the natural climate variability i.e. climate volatility. Climate change and climate volatility has many observed impacts, and for a full list of the observed impacts see Pörtner et al. [2022].

Since the countries of G7 and BRIC is responsible for most of the global CO_2 emission, it could be interesting to examine, if the climate volatility is dependent on the financial volatility. Since the BRIC countries produce 20% percent point more than the G7 countries, it is expected that the climate volatility would be more dependent on the financial market of BRIC than the G7. As mentioned before in order to measure the financial market of G7, this thesis will focus on the Standard and Poor's 500 (S&P 500) index. Furthermore in order to measure the financial market of the countries of BRIC, this thesis will focus on the MSCI BRIC index. Daily observations of the S&P 500 index is once more presented below.

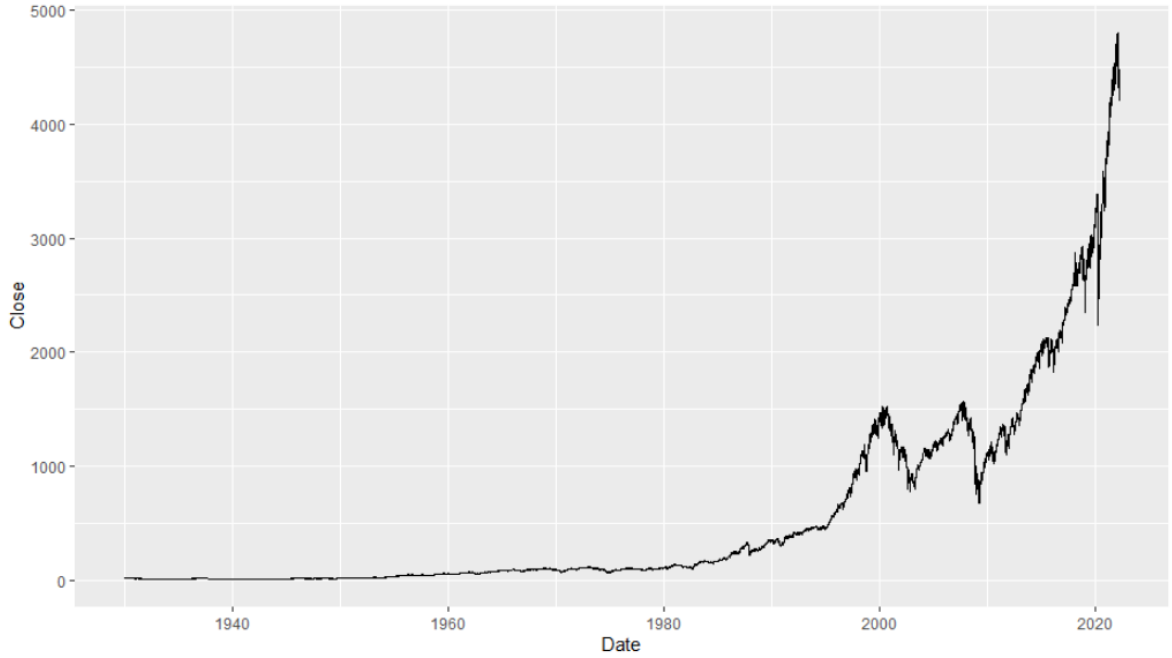

Figure 4.3. Daily observations of the S&P 500 index from 1930-2022.

The S&P 500 is a stock market index, which is tracking the performance of 500 large companies[2] listed on stock exchanges in the United States. The time series consist of daily data from the S&P 500 index, which has the variables open, high, low and close. The dataset can be extracted from DataHub [2022] starting at 1930-01-01 and ending in 2022-01-03. The high and low price indicates respectively the maximum and minimum prices in a given time period. The open and close prices indicates respectively the prices at which a stock began and ended trading in the same period. In this thesis, the closing price is considered and it is given in figure 4.3.

The MSCI BRIC index is a free float-adjusted market capitalization weighted index, which is designed to measure the equity market performance across the BRIC countries. MSCI is an acronym for Morgan Stanley Capital International, which is an investment research firm, that provides stock indexes, portfolio risk and performance analytics and governance tools to institutional investor and hedge funds[3]. Therefore as mentioned before this thesis will focus of the MSCI BRIC index in order to measure the financial market of the BRIC. Daily observations of the MSCI BRIC index is once more presented below.

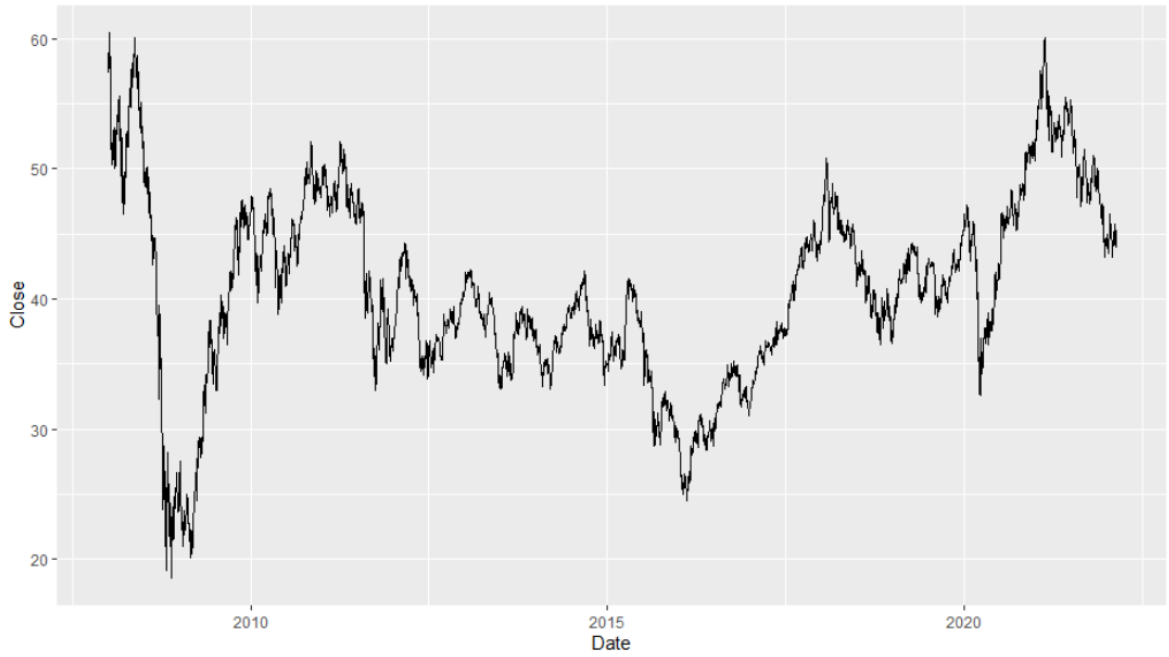

Figure 4.4. Daily observations of the MSCI BRIC index from 2008-2022.

The MSCI BRIC index consist of daily observation with the variables open, high, low and close. This data can be extracted from finance [2022] starting in 2008-01-01 and ending on 2021-12-31. This thesis will be limited to the closing price, which is given in figure 4.4.

[2]For a full list of companies in the S&P 500 see Slickcharts [2022]
[3]See MSCI [2019] for more information

4.3 Data adjustment

In order to answer the question of the dependence structure of the different measures, it is required that the compared time series need to have the same length. This section is used in order to both depict which time series to compare and to determine the length of the individual time series.

When observing the CO_2 emission given in figure 4.2 on page 21, it can be observed, that the CO_2 emission was increasing ca. in the period of 1950-1970 for the countries of G7. Furthermore does the CO_2 emission for the countries of the BRIC seem to be increasing throughout the whole period 1950-2020. Inspecting the temperature anomalies on figure 4.1 on page 19, it looks like they also have been increasing from ca. 1970 and forward. It would therefore be interesting to firstly examine the dependency structure of the modelled climate- and G7 volatility measure, secondly the modelled climate- and BRIC volatility measure to get an insight in the individual effect. Lastly the combined modelled climate-, G7- and BRIC volatility measures could be of interest, to get an insight of the combined effect. These three models will be the focus of this thesis.

Now that it is clear which time series to compare, the time series should be constructed such that they have the same length. The range of the temperature anomalies is from 1880-01-01 to 2021-12-31, the range of the closing prices of the $S\&P$ 500 index is from 1930-01-01 to 2021-01-03 and the range of the closing prices of the MSCI BRIC index is from 2008-01-01 to 2021-12-31. To keep the length of the three time series consistent, the range of all three time series is set from 2008-01-01 to 2021-12-31.

The first group of time series concentrates on the effect of the temperature anomalies on the financial market from the G7 countries, namely the closing price of the $S\&P$ 500 index. This comparison is given in the following figure.

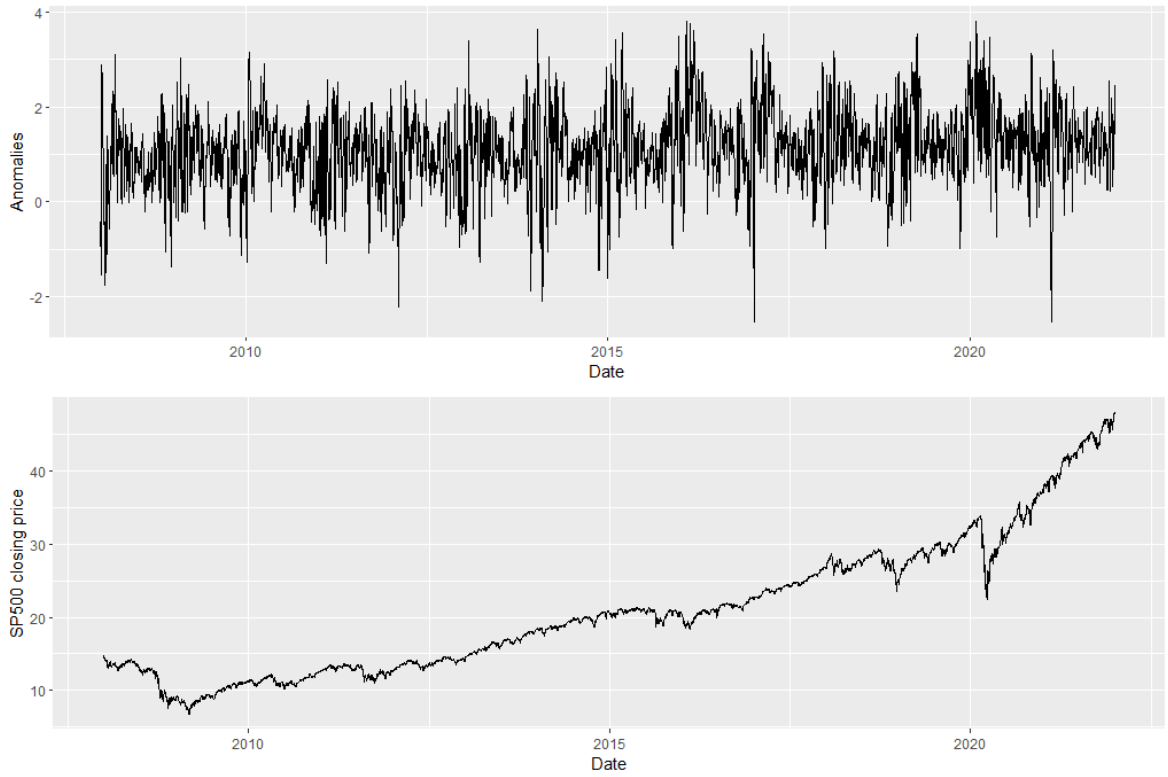

Figure 4.5. The adjusted time series from the comparison of the temperature anomalies and the $S\&P$ 500 index.

The adjusted times series given figure 4.5 will from now on be referred to as C-SP.

Secondly the effect of the temperature anomalies on the financial market from the BRIC countries is of interest. The comparison of the two time series starts in 2008-01-01 and ends on 2021-12-31, which is shown in the following figure.

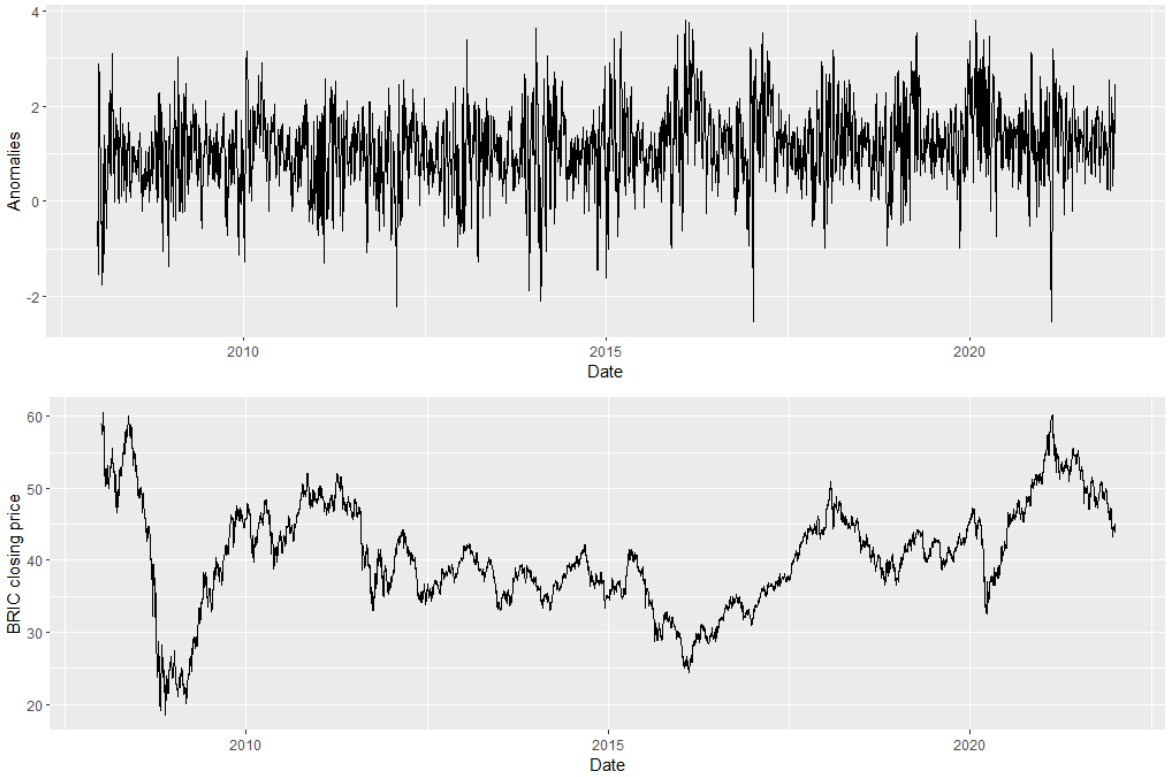

Figure 4.6. The adjusted time series adjusted to the comparison of the temperature anomalies and the financial market of the BRIC index.

The adjusted times series given figure 4.6 will from now on be referred to as C-BRIC.

The last comparison is between all of the three time series. The comparison consisting of the three time series is shown in the following figure.

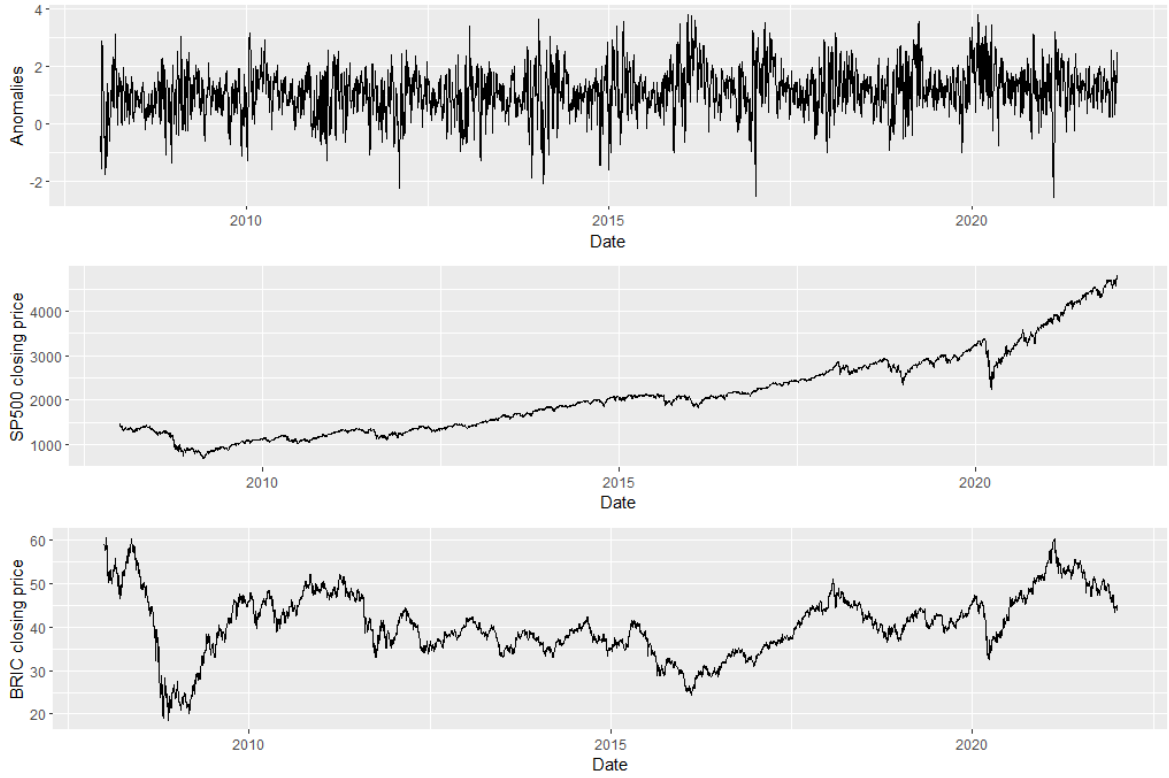

Figure 4.7. The adjusted time series adjusted to the comparison of the temperature anomalies and both the financial markets.

The adjusted times series given figure 4.7 will from now on be referred to as C-SP-BRIC.

Chapter 5

Modelling

In this chapter a linear deterministic seasonality model is constructed on the data of temperature anomalies, the S&P 500 index and the MSCI BRIC index in the period 2008-2022. Next using the residuals, the steps and results involved in modelling the TVP-VAR-SV model will be presented. The theory used in this chapter can be found in chapter 2 on page 5 and chapter 3 on page 15 if not stated otherwise.

If the dataset exhibit seasonality, this should be accounted for before the analysis of TVP-VAR-SV. In this thesis it will be assumed, that the data exhibit deterministic seasonality, which will be accounted for in the following section. This thesis will focus on estimating the deterministic seasonality.

5.1 Deterministic Seasonality

Inspecting figure 4.5, figure 4.6 and figure 4.7 on respectively page 25, page 26 and page 27, it can be argued, that they exhibit some kind of seasonality. It can furthermore be argued, that they exhibit some kind of trend. In order to further check for seasonality and trend, Escribano et al. [2011] suggest the following seasonality function:

$$\begin{aligned} P_t = \gamma_0 + t\gamma_1 &+ C_1 sin(2\pi t/7) + C_2 cos(2\pi t/7), && \textit{(Weekly)} \\ &+ C_3 sin(2\pi t/(K/4)) + C_4 cos(2\pi t/(K/4)), && \textit{(Quarterly)} \\ &+ C_5 sin(2\pi t/(K/2)) + C_6 cos(2\pi t/(K/2)), && \textit{(Semi-annual)} \\ &+ C_7 sin(2\pi t/K) + C_8 cos(2\pi t/K), && \textit{(Annual)} \end{aligned}$$

where γ_0 is a intercept constant, γ_1 is the trend coefficient, $C_1, \ldots, C_8$ are the coefficients for the annual cycle. Here the constant K determines the number of observations given in a year, which is number of days given in a year i.e. 365.25. This linear model is estimated using the method of Ordinary Least Squares (OLS). Thus a p-value can be calculated for each corresponding parameter. If the p-value is below 0.05 the parameter is set to 0. Thus resulting in the following parameters for temperature anomalies, the closing price of S&P 500 index and the MSCI BRIC index:

	Anomalies	S&P 500	MSCI BRIC
γ_0	$8.354e-01$	587.13	38.41
γ_1	$1.132e-04$	0.588	$8.456e-04$
C_1	0	0	0
C_2	0	0	0
C_3	0	0	$3.280e-01$
C_4	$7.086e-02$	0	0
C_5	0	0	0
C_6	$-1.240e-01$	13.24	0
C_7	$2.341e-01$	0	$6.862e-01$
C_8	0	0	$-3.779e-01$

Table 5.1. Parameter values from the linear deterministic seasonality model.

Using those parameters, the corresponding residuals given from these linear models is displayed in the following figures:

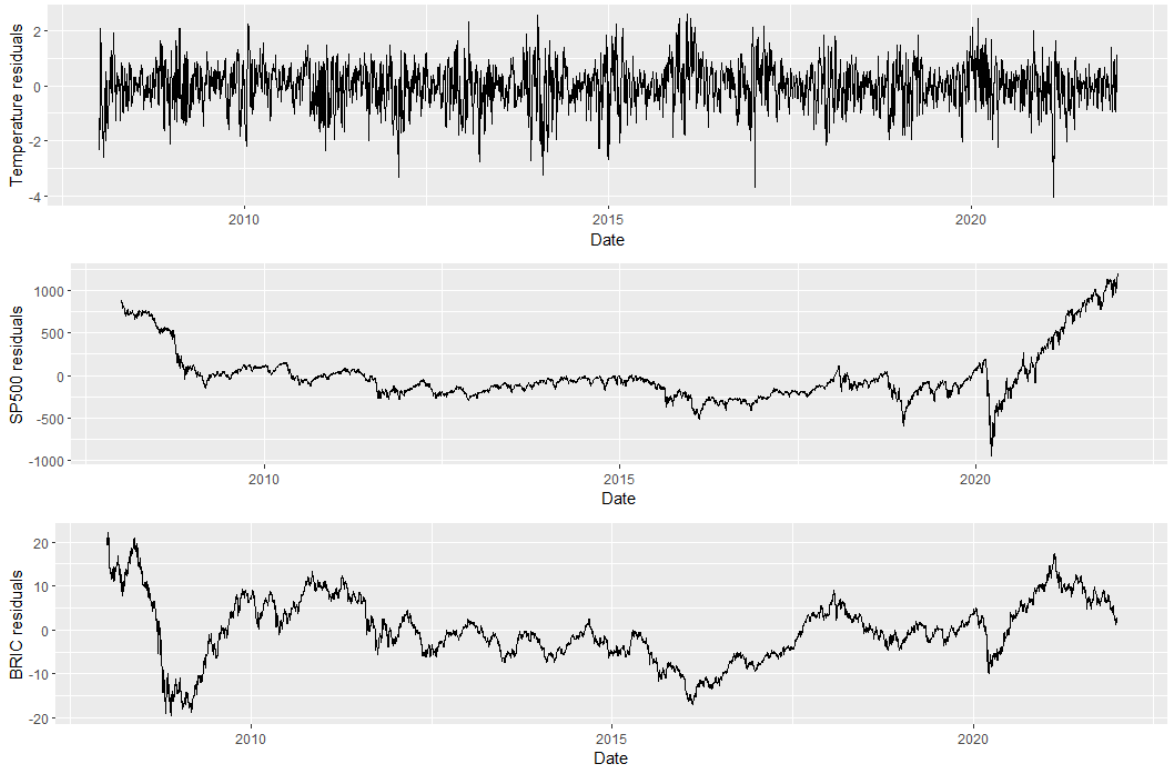

Figure 5.1. The residuals from using the linear model on temperature anomalies, the S&P 500 index and the MSCI BRIC index.

The groups obtained when inserting the residuals into the comparison groups will be referred to as Res-C-SP, Res-C-BRIC and Res-C-SP-BRIC.

Now using the residual from the linear deterministic seasonal model, the initial settings for the model TVP-VAR-SV needs to be determined.

5.2 Model construction

As described in chapter 4 on page 19 the techniques of Bayesian Inference used in TVP-VAR-SV are applied for the estimation of the data Res-C-SP, Res-C-BRIC and Res-C-SP-BRIC. For the estimation of the TVP-VAR-SV model one lag is used. Furthermore the simulations used in the Gibbs sampler are based on 50.000 iterations, where the first 5.000 samples are discarded for convergence. Thus to summarize the initial settings of the model is:

- $s = 1$
- $nrep = 50.000$
- $nburn = 5.000$

Now that the construction of the initial settings of the model, the initial settings of the priors needs to be determined.

5.2.1 Priors

The first two years will be used for calibration of the prior distributions, meaning 731 observations from 2008-2010. Furthermore the mean of B_0 for the models Res-C-SP and Res-C-BRIC is chosen to be the OLS point estimates[1] ($\hat{B}_{OLS}$) and the variance of B_0 is chosen to be three times its variance in a time invariant VAR estimated on the small initial sub sample. The mean of B_0 for the model Res-C-SP-BRIC is also chosen to be the OLS point estimate, however the variance are chosen to be four times its variance in a time invariant VAR estimated on the small initial sub sample. It should be noted, that the multiplied constants three and four is determined by the dimension of each matrix plus one accordingly to E. Primiceri [2005]. A reasonable prior for A_0 can be obtained in the same way. The mean of h_0 is also chosen to be the OLS point estimate ($\hat{h}_{OLS}$), however the variance matrix is assumed to be the identity matrix.

The prior distribution of the hyperparameters are assumed to follow the inverse-Wishart distribution. Thus the degrees of freedom and scale matrices are needed. The degrees of freedom are set to be three for W and S for model Res-C-SP and Res-C-BRIC and set to be four for W and S for model Res-C-SP-BRIC. The degrees of freedom is chosen as such, since they must exceed the dimension of respectively W and S for the inverse-Wishart distribution to be proper. Therefore since the size of the previous initial sub sample is 731, this will also be the degrees of freedom for Q.

Summarizing, the priors from the models Res-C-SP and Res-C-BRIC take the form:

$$
\begin{aligned}
B_0 &\sim \mathcal{N}\left(\widehat{B}_{OLS}, 3 \cdot Var\left(\widehat{B}_{OLS}\right)\right), \\
A_0 &\sim \mathcal{N}\left(\widehat{A}_{OLS}, 3 \cdot Var\left(\widehat{A}_{OLS}\right)\right), \\
h_0 &\sim \mathcal{N}\left(\log\left(\widehat{h}_{OLS}\right), I_n\right), \\
Q &\sim IW\left(k_Q^2 \cdot 731 \cdot Var\left(\widehat{B}_{OLS}\right), 731\right), \\
S &\sim IW\left(k_S^2 \cdot 3 \cdot Var\left(\widehat{A}_{OLS}\right), 3\right), \\
W &\sim IW\left(k_W^2 \cdot 3 \cdot I_n, 3\right),
\end{aligned}
$$

And the priors from the model Res-C-SP-BRIC take the form:

$$
\begin{aligned}
B_0 &\sim \mathcal{N}\left(\widehat{B}_{OLS}, 4 \cdot Var\left(\widehat{B}_{OLS}\right)\right), \\
A_0 &\sim \mathcal{N}\left(\widehat{A}_{OLS}, 4 \cdot Var\left(\widehat{A}_{OLS}\right)\right), \\
h_0 &\sim \mathcal{N}\left(\log\left(\widehat{h}_{OLS}\right), I_n\right), \\
Q &\sim IW\left(k_Q^2 \cdot 731 \cdot Var\left(\widehat{B}_{OLS}\right), 731\right), \\
S &\sim IW\left(k_S^2 \cdot 4 \cdot Var\left(\widehat{A}_{OLS}\right), 4\right), \\
W &\sim IW\left(k_W^2 \cdot 4 \cdot I_n, 4\right),
\end{aligned}
$$

The results of the constructed models are obtained using the values $k_Q = 0.01$, $k_S = 0.1$ and $k_W = 0.01$. For a detailed discussion of this choice, the robustness of the results to alternative prior specifications and the choice of Q see E. Primiceri [2005,p. 19-22].

[1] See Mahaboob et al. [2018,p. 518-520] for details of point estimates.

Now that the prior is specified, it is possible to use the residuals, Res-C-SP, Res-C-BRIC and Res-C-SP-BRIC in the implementation of the TVP-VAR-SV model.

5.3 Implementation

Firstly the model is implemented using the residuals Res-C-SP. Next the posterior stochastic volatility is extracted, which results in the following figures.

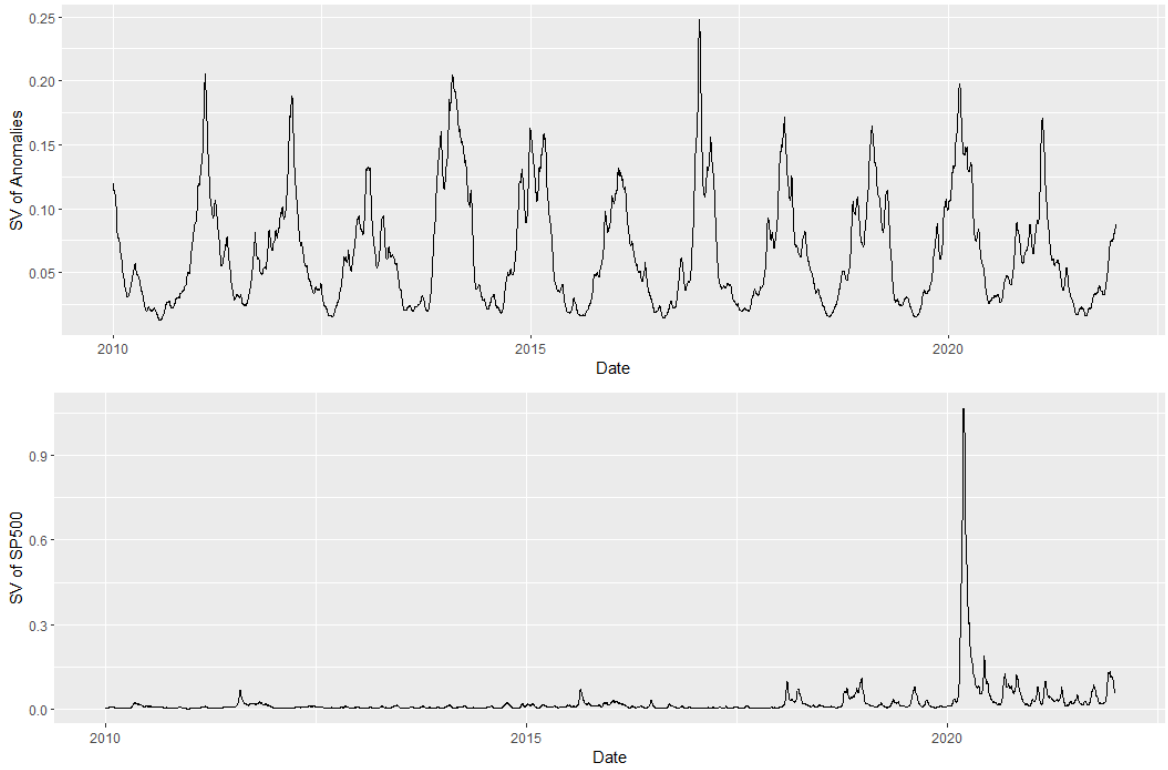

Figure 5.2. Stochastic Volatility from TVP-VAR-SV using Res-C-SP in the period 2008-2022.

Notice that even though the period of the residuals for Res-C-SP is 2008-2022, the period of the stochastic volatility is from 2010-2022 due to the priors using the first 2 years for calibration. Furthermore in the start of 2020, the epidemic COVID-19 were happening across the world. This can clearly be observed in the stochastic volatility for the $S\&P$ 500 index. In the same period the stochastic volatility for the temperature anomalies seem to be risen as well. However it seems to be stabilizing the next year.

Next the model is implemented using the residuals Res-C-BRIC, where the posterior stochastic volatility is extracted, and presented in the following figures.

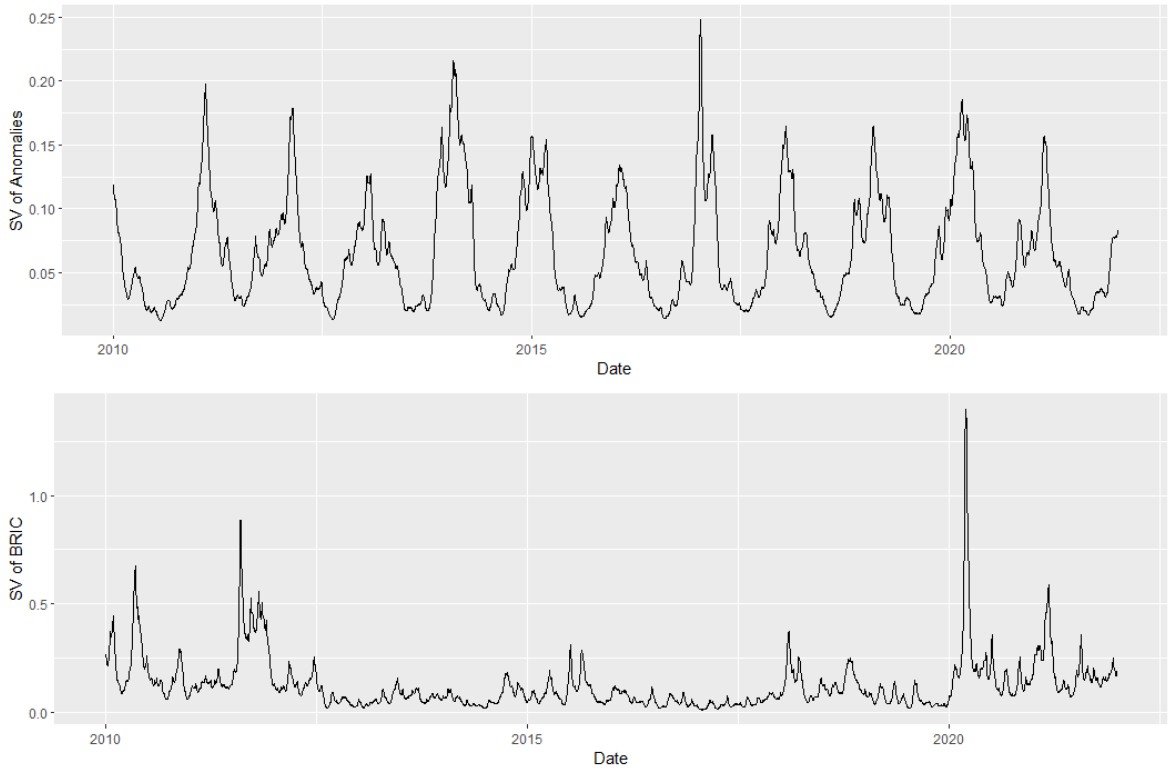

Figure 5.3. Stochastic Volatility from TVP-VAR-SV using Res-C-BRIC in the period 2008-2022.

As before the period of the stochastic volatility for Res-C-BRIC is from 2010-2022 due to the 2 year calibration. The epidemic can likewise be observed in the stochastic volatility for the MSCI BRIC index with the spike in the start of 2020. It can furthermore be seen, that there were a lot of spikes in the stochastic volatility of the MSCI BRIC index in the period 2010-2013. The effect of this on the temperature volatility is not immediately. However it looks like the temperature volatility is lower in the year 2013. This effect will be further elaborated upon later.

Lastly the model is implemented using the residuals Res-C-SP-BRIC, where the posterior stochastic volatility is extracted and presented in the following figures.

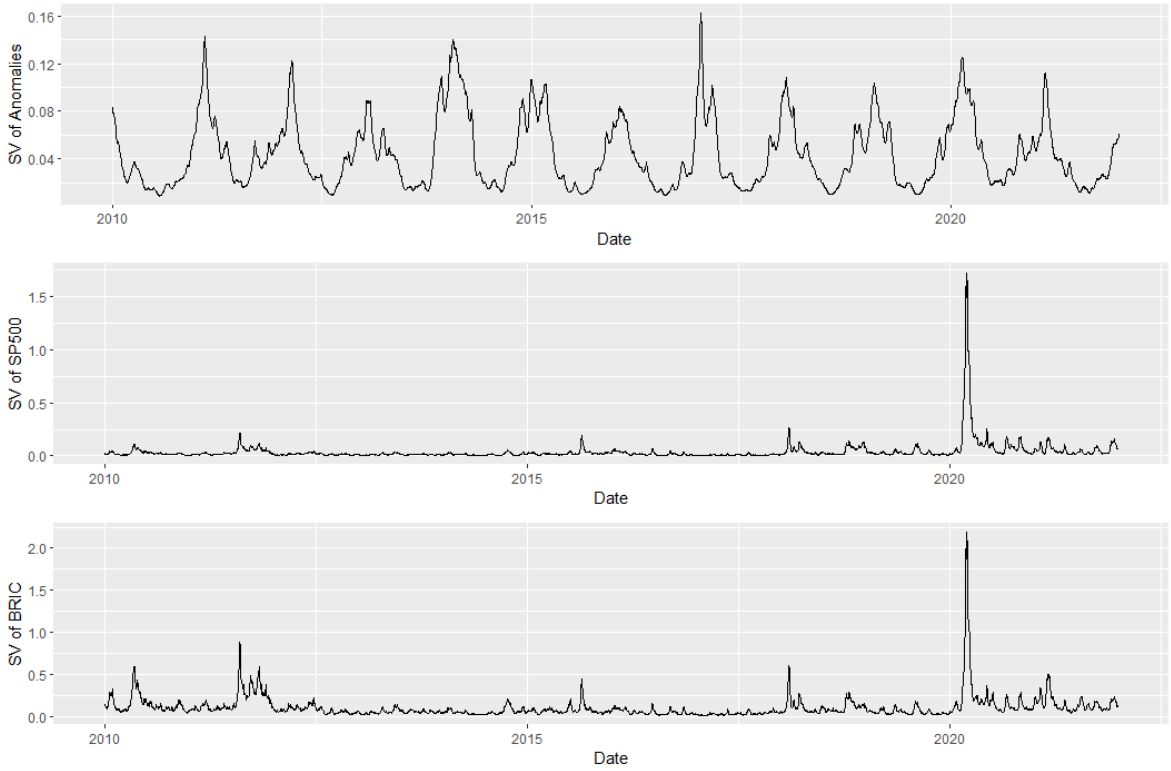

Figure 5.4. Stochastic Volatility from TVP-VAR-SV using Res-C-SP-BRIC in the period 2008-2022.

Again the period of the stochastic volatility for Res-C-SP-BRIC is from 2010-2022 due to the 2 year calibration. Here the period of COVID-19 can be observed for both financial volatility measures with the spikes in the start of 2020. However the spikes is increased in size from ca. 1 to 1.6 and 1.8 to 2.1 for the volatility of respectively the S&P 500 and MCSI BRIC index.

When modeling the groups of residuals an interesting result is the financial volatility spikes in the start of 2020. This lead to the question of the effect of the epidemic, and it could therefore be interesting to calculate the stochastic volatility before the epidemic COVID-19. This will be examined in the following section.

5.4 Implementation before COVID-19

Firstly the model is implemented using the residuals Res-C-SP in the period 2008-2020. Next the posterior stochastic volatility is extracted, which results in the following figures.

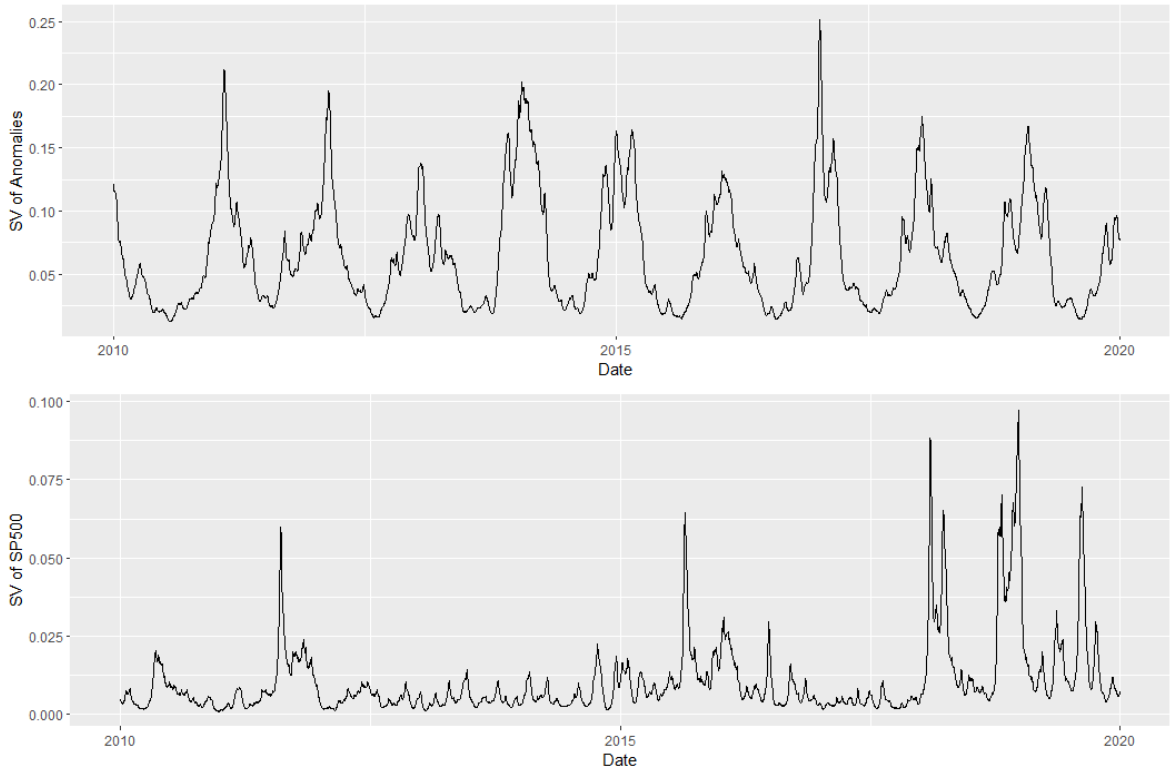

Figure 5.5. Stochastic Volatility from TVP-VAR-SV using Res-C-SP in the period 2008-2020.

The stochastic volatility of Res-C-SP before COVID-19 ranges from 2010 to 2020. It can be observed that the temperature volatility has a large spike in 2017, where the volatility of S&P 500 looks to be almost stable. However in the years 2015-2016 the S&P 500 volatility was high, which could have been the resulting factor for the low temperature volatility in 2016. Furthermore at 2011-2012 there was a large spike in the volatility of S&P 500, where a decrease in temperature volatility is happening 2012 and 2013. Lastly the years 2018-2020 seem to have been very volatile resulting in no observable immediately effect on the temperature volatility.

Secondly the model is implemented using the residuals Res-C-BRIC in the period 2008-2020, the posterior stochastic volatility is extracted, and then presented in the following figures.

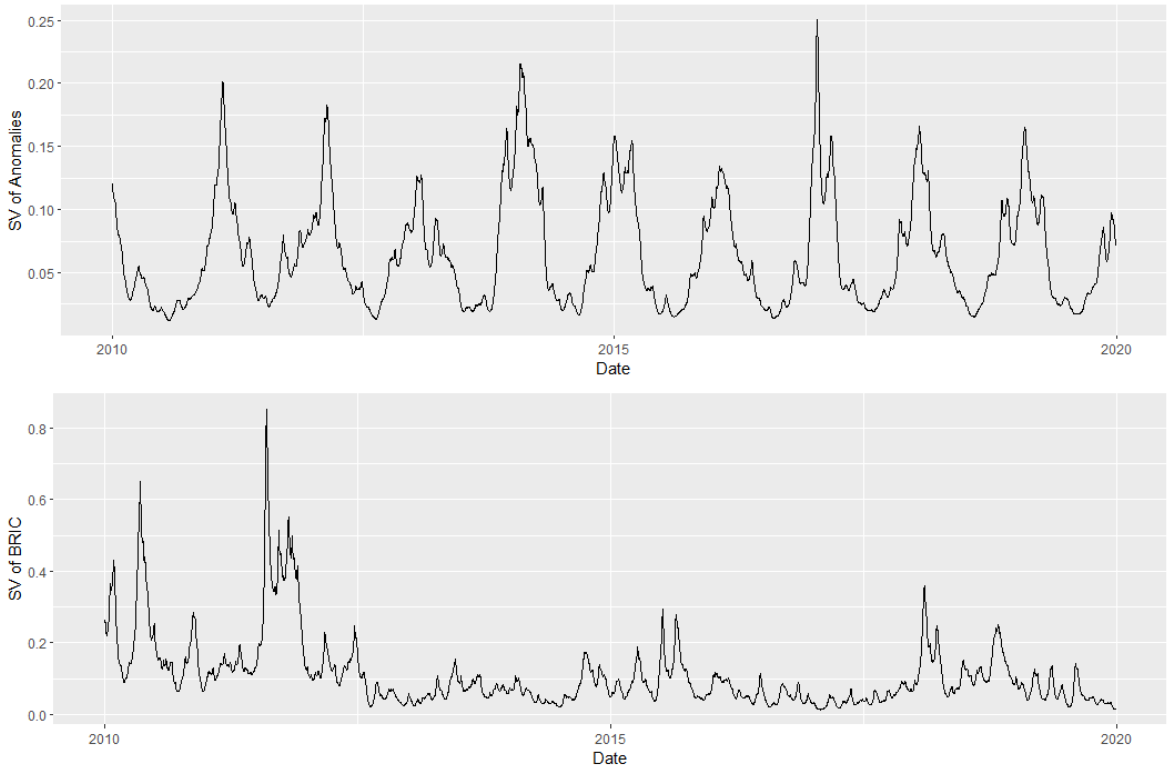

Figure 5.6. Stochastic Volatility from TVP-VAR-SV using Res-C-BRIC in the period 2008-2020.

It can be observed, that the volatility of MSCI BRIC index spikes in the years 2011-2012, where the temperature volatility is decreasing until year 2013. Furthermore like in figure 5.5 on 34, there is also a little increase in the MSCI BRIC volatility the years 2014-2016, which could have been the resulting factor for the decrease in temperature volatility observed in year 2016.

Lastly the model is implemented using the residuals Res-C-SP-BRIC in the period 2008-2020, where the posterior stochastic volatility is extracted[2]. However apart from a slightly increase in the S&P 500 volatility, the figures 5.6 and 5.5 on representative page 35 and page 34 are very much alike.

One of the main results from this section was, that the stochastic volatility constructed from S&P 500 and temperature anomalies might exhibit *lagged dependency* between each other. Furthermore the stochastic volatility constructed from the MSCI BRIC index and temperature anomalies might also exhibit this kind of dependency between each other. In order to measure such dependency, Timothy and Joshua [2004] suggest to use *Cross-correlation*. Cross-correlation is used in order to explore how one time series may predict or explain another time series.

[2]See figure A.1 on page A.1.

5.5 Cross Correlation

Given two time series x_t and y_t, where $t = 1, \ldots, n$, and where x_t is delayed by T samples, then it is possible to calculate the *cross-covariance*. This is defined as

$$\sigma_{xy}(T) = \frac{1}{n-1} \sum_{i=1}^{n} (x_{i-T} - \mu_x)(y_i - \mu_y),$$

where μ_x and μ_y are the means of respectively x_t and y_t. Now using the cross-covariance, it is possible to calculate the *cross-correlation* as

$$\rho_{xy}(T) = \frac{\sigma_{xy}(T)}{\sqrt{\sigma_{xx}(0)\sigma_{yy}(0)}},$$

where $\sigma_{xx}(0)$ and $\sigma_{yy}(0)$ is clearly just the variance of respectively x_t and y_t due to no sample delay[3].

5.5.1 Cross-correlation including COVID-19

In order to capture the lagged dependency, the Cross-correlation between the calculated climate and financial volatility measures is modelled. The Cross-correlation between the volatility of S&P 500 index and temperatures will be denoted as CCF-SP-C, and the Cross-correlation between the volatility of MSCI BRIC index and temperature will be denoted as CCF-BRIC-C. Firstly the Cross-correlation is calculated for the volatility measures calculated from Res-C-SP and Res-C-BRIC in the period including COVID-19. The resulting figures of CCF-SP-C and CCF-BRIC-C with the maximum values of T set to 100 is given as.

[3]For further information of Cross-correlation see Timothy and Joshua [2004]

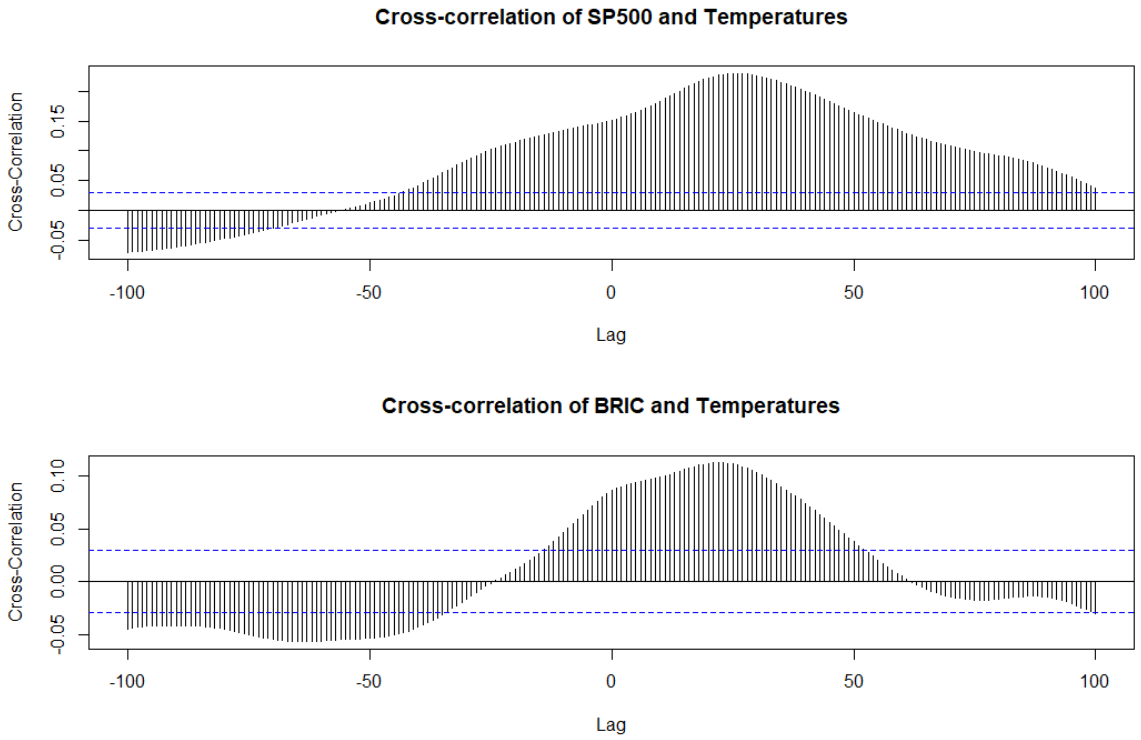

Figure 5.7. Cross-correlation using the stochastic volatility of Res-C-SP and Res-C-BRIC with $max(|T|) = 100$.

The blue dotted line indicates the 95% confidence interval. The CCF-SP-C indicates, that the measures are correlated at lag 0. However the Cross-correlation increase until ca. 25 days after reaching a maximum. The same result appears for CCF-BRIC-C. This indicates, that the financial volatility measures is correlated with the climate volatility measure, even though the size of the correlation seems small. This result will be further elaborated upon later.

In order to observe the long term Cross-correlation, the CCF-SP-C and the CCF-BRIC-C is calculated for respectively Res-C-SP and Res-C-BRIC in the period 2010-2022 with the maximum values of T set to 700. This is displayed in figure A.2 on page 56. The CCF-SP-C shows a positive correlation roughly each ± 365 days, and a negative correlation roughly in between, thus indicating a seasonal correlation. Here the CCF-BRIC-C shows mostly a negative correlation at almost all past lags, a positive yearly correlation at future lags and a negative correlation in the 500-700 lag period. This will be further elaborated upon later.

Next the dependency of the full model, namely Res-C-SP-BRIC, is examined, in order to observe if the result of the full model differ from the result of the divided models. The CCF-SP-C and CCF-BRIC-C is then calculated again with the maximum values of T set to 100. The result is given in the following figures.

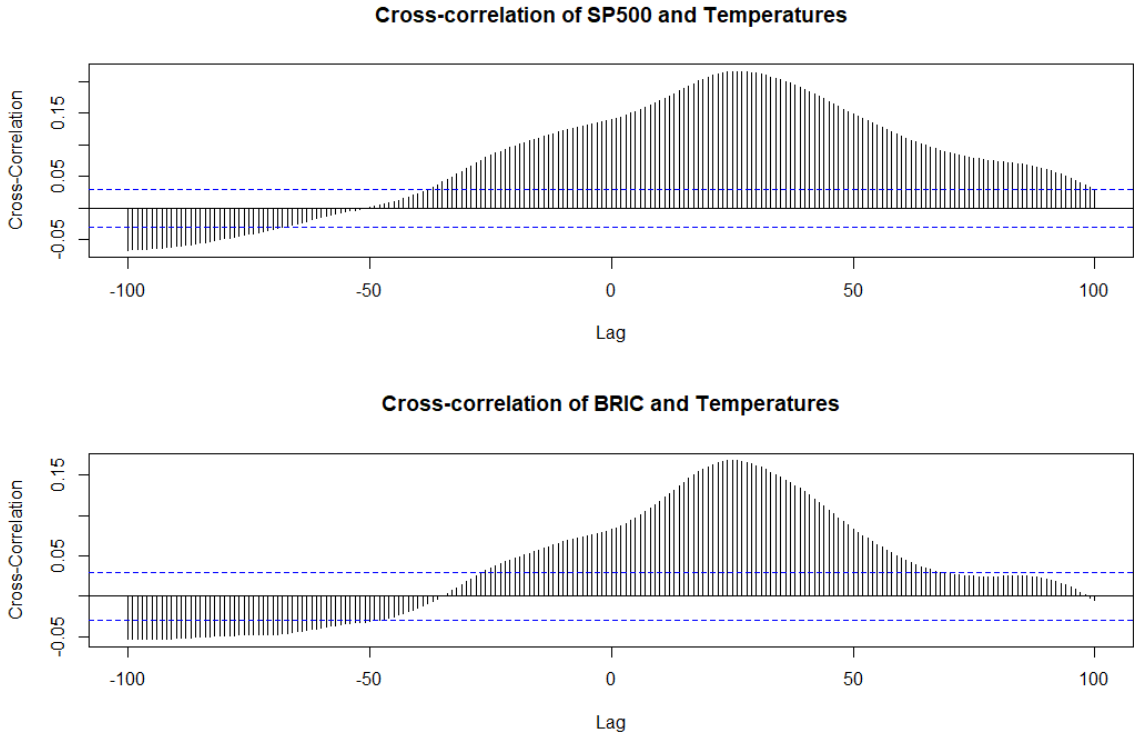

Figure 5.8. Cross-correlation using the stochastic volatility of Res-C-SP-BRIC with $max(|T|) = 100$.

Again the dotted line represents the 95% confidence interval. The CCF-SP-C given in figure 5.8 is almost identical figure 5.7 on page 37, thus indicating that the volatility of BRIC have no effect in the correlation between the volatility of S&P 500 and temperatures. The CCF-BRIC-C does however differs, where at ca. the 25 lag the Cross-correlation has risen ca. 5 percentage point. This indicates, that the volatility of S&P 500 have a impact in this model, when calculating the CCF-BRIC-C.

As before in order to observe the long term Cross-correlation, the CCF-SP-C and the CCF-BRIC-C is calculated for Res-C-SP-BRIC in the period 2010-2022 with the maximum values of T set to 700. This is displayed in figure A.3 on page 57. Both the CCF-SP-C and the CCF-BRIC-C shows a positive yearly correlation, and a negative correlation at the lags in between. This is interesting since the volatility of the MSCI BRIC index has become more seasonal correlated, when modelled with the S&P 500 index.

As mentioned the epidemic COVID were happening in the start of 2020 showing spikes of the financial volatility. Thus in order to observe the effect of the epidemic COVID-19 on the lagged dependency, the Cross-correlation of the period before this epidemic is calculated.

5.5.2 Cross Correlation before COVID-19

As before the CCF-SP-C and CCF-BRIC-C is firstly calculated for Res-C-SP and Res-C-BRIC in the period 2010-2020. However this time the maximum values of T is set to 700 to capture the yearly correlation effect. The result is given in the following figures.

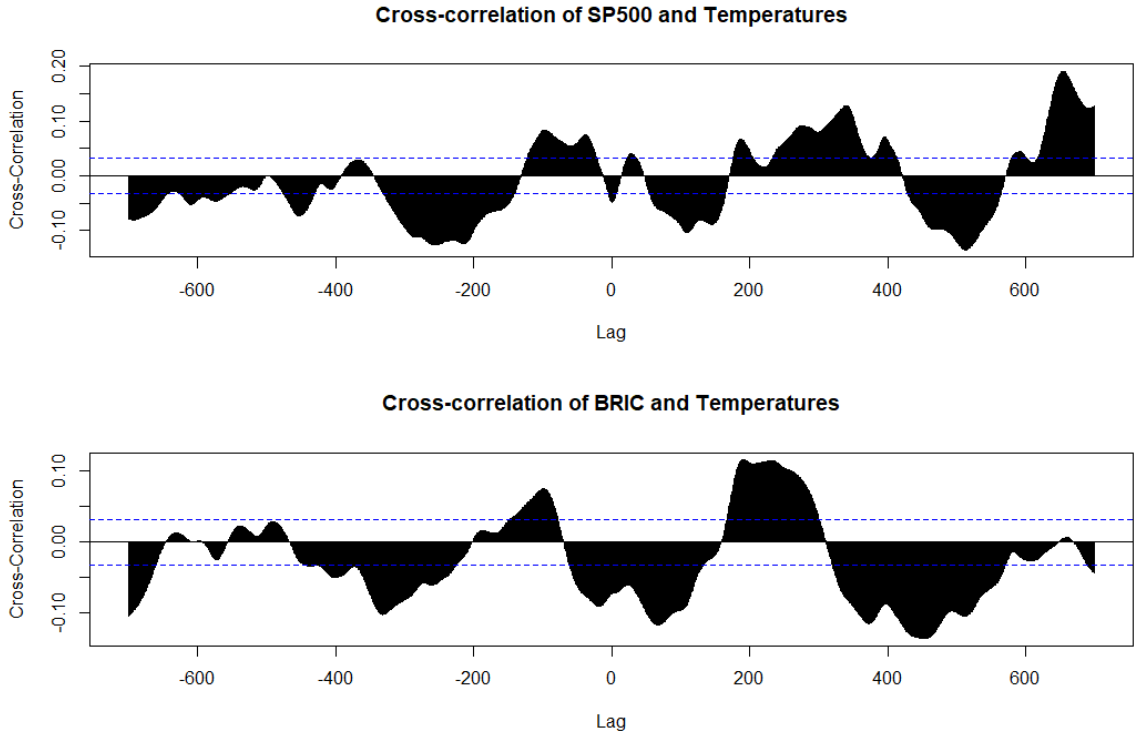

Figure 5.9. Cross-correlation using the stochastic volatility of Res-C-SP and Res-C-BRIC with $max(|T|) = 700$ in 2010-2020.

The CCF-SP-C shows the maximum Cross-correlation absolute value at around the $600-700$ lag. This indicates, that the volatility of the S&P 500 index is correlated with the climate volatility calculated almost at the 2 year mark. However the CCF-BRIC-C shows the maximum Cross-correlation absolute value at around the 200 lag and at the 350-500 lag period. This indicates, that the volatility of MSCI BRIC is correlated with the climate volatility calculated after half a year and after one year.

In order to observe the short term Cross-correlation, the CCF-SP-C and the CCF-BRIC-C is calculated for Res-C-SP and Res-C-BRIC in the period 2010-2020 with the maximum values of T set to 100. This is displayed in figure A.4 on page 58. The CCF-BRIC-C is mostly negative throughout the period. However ca. from lag -100 to lag -70 it actually shows a positive correlation. The CCF-SP-C shows a varying correlation, where it is positive at past lags and negative at lag 50 and forward.

Lastly the CCF-SP-C and CCF-BRIC-C is calculated for Res-C-SP-BRIC in the period 2010-2020 with maximum values of T set to 700. The result is given in the following figures.

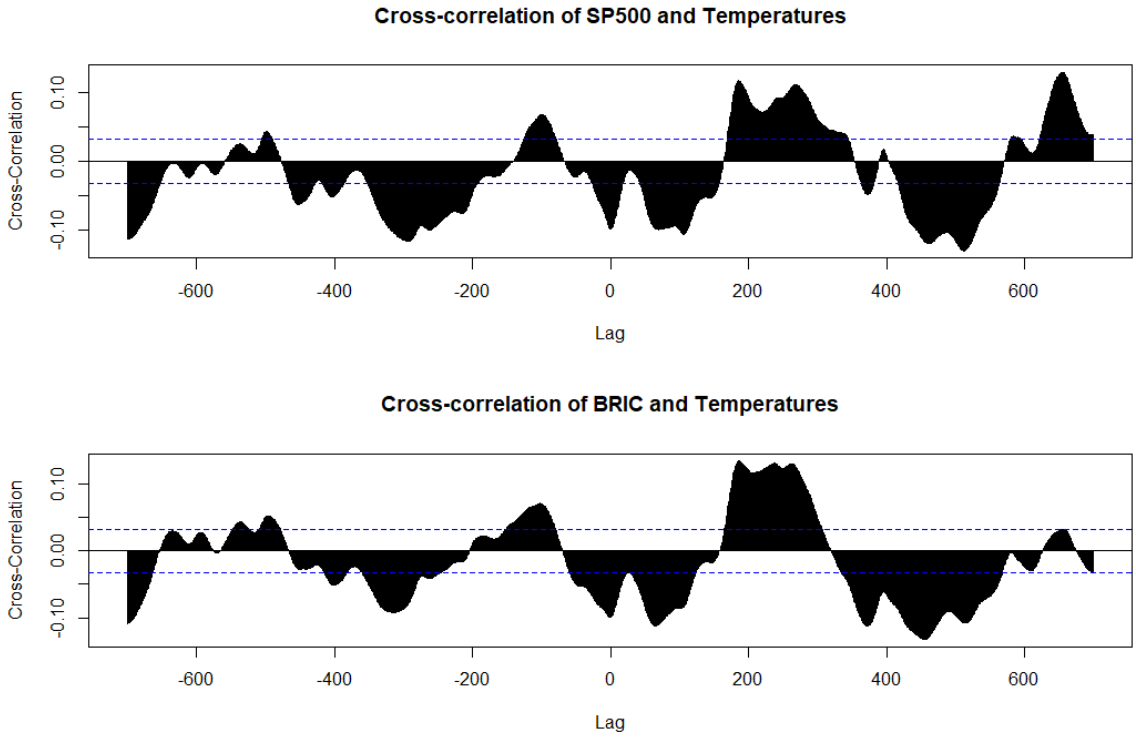

Figure 5.10. Cross-correlation using the stochastic volatility of Res-C-SP-BRIC with $max(|T|) = 700$ in 2010-2020.

The CCF-BRIC-C here is almost identical to figure 5.9 on page 39, and as before, the CCF-SP-C shows a correlation after 600 lags. However a correlation at the 150-300 lag period and at around the 500 lag is added. This indicates, that there is a ca. half yearly, one and a half yearly and a double yearly effect on volatility of S&P 500 index from the climate volatility.

Now as before in order to observe the short term Cross-correlation, the CCF-SP-C and the CCF-BRIC-C is calculated for Res-C-SP-BRIC in the period 2010-2020 with the maximum values of T set to 100. This is displayed in figure A.5 on page 59. Most interesting is that where the CCF-BRIC-C seems almost unchanged, the CCF-SP-C has taken some aspects from the volatility of the MSCI BRIC index when calculating the Cross-correlation.

The Cross-correlation is calculated between the volatility of S&P 500 and the volatility of MSCI BRIC index from Res-C-SP-BRIC, which can be seen in section A.2.3 on page 60. Both the Cross-correlation from 2008-2022 and 2008-2020 indicates, that there is a clear dependency between the financial volatility measure of S&P 500 and the BRIC. This dependency is most clearly at the period between the -50 lag and the 50 lag. Since the S&P 500 index and the MSCI BRIC index individually makes up a huge part of the global financial market, the dependency between those financial markets is not surprising.

5.6 Diagnostics and additional interpretation

Now that the results of the model construction and the implementation where the dependence structure afterwards has been shown, this section will be used for further diagnostics and interpretation of the results.

The Cross-correlation has now been calculated, however further examination is needed. When modelling the full data, i.e. Res-SP-BRIC, it was observed, that the CCF-SP-C achieved properties from the CCF-BRIC-C and vice versa. Thus modelling on the full data and calculating the Cross-correlation might result the volatility index being more correlated, than they are in reality. Therefore since this thesis focus individually on the CO_2 emission effect of respectively the BRIC and the G7 on the climate volatility measure, this section will focus on the CCF-SP-C and the CCF-BRIC-C calculated for respectively Res-C-SP and Res-C-BRIC.

The Cross-correlation coefficient ranges from -1 to 1, where a value of exactly 1 means, that there is a perfect positive relationship between the two variables, and a value of exactly -1 means, that there is a perfect negative relationship between the two variables. When the Cross-correlation coefficient is exactly 0, it means, that there is no relationship between the two variables. Thus Cross-correlation can be used to explore, how one time series may predict or explain another.

The S&P 500 index and the MSCI BRIC index is describing respectively 500 corporations and four countries. Thus the volatility of those indexes is dependent on loads of factors. Furthermore the temperature anomalies, and thus the climate volatility, is also dependent on loads of factors. Since the climate and financial volatility measures covers large and different areas, it should be expected, that the CCF-SP-C and CCF-BRIC-C does not reach values close to ± 1. Therefore any Cross-correlation coefficient value beyond the blue dotted confidence interval line is assumed to be significant.

Now in order to use the Cross-correlation to interpret the relationship between the climate volatility measure and the financial volatility measure, firstly focus on figure 5.7 on page 37. From those figures one can deduce, that the climate volatility measure is more positively correlated with the volatility of the S&P 500 index than with the volatility of the MSCI BRIC index in the short term. This means that the climate volatility measure increases or decreases more, when the volatility of the S&P 500 index respectively increases or decreases, than if the volatility of the MSCI BRIC index respectively increases or decreases. To summarize this means, that including the period of COVID-19, the CCF-SP-C and CCF-BRIC-C indicates, that the difference in CO_2 emission does not have an observed effect on the climate volatility measure in the short term.

Secondly for the long term effect the focus is figure A.2 on page 56 which includes the period of COVID-19. As mentioned before both the CCF-SP-C and the CCF-BRIC-C indicates a seasonal correlation. However the climate volatility seems to be more negatively correlated with the volatility of the MSCI BRIC index, than with the volatility of the S&P index. This indicates, that if the volatility of the S&P 500 index or MSCI BRIC index changes, it will have a long term seasonal effect on the climate volatility. Observing figure 5.6 on page 35 this effect can clearly been seen, since after a volatility spike from the MSCI BRIC index in year 2011-2012, the temperature volatility is reduced a lot in year 2013. Same result can be

observed for the volatility of the S&P 50 index using the figure 5.5 on page 34.

Thirdly for the short term effect in the period before COVID-19, lets focus on figure A.4 on page 58. The most interesting aspect of the Cross-correlation in this period is how different it is from the Cross-correlation in the period including the COVID-19. This could indicate, that the financial volatility spike changes the Cross-correlation of the volatility measures, such that it might not be representative for the period before COVID-19 in the short term. Furthermore in the short term, there seems to be fluctuations. Both aspects will be further investigated, when observing the long term effect.

Lastly for the long term effect in the period before COVID-19, lets focus on figure 5.9 on page 39. As in the period including COVID-19, the CCF-SP-C exhibit almost the same seasonal correlation pattern, where the relationship is more positive correlated each year, and is more negative correlated in between, where the CCF-BRIC-C exhibit the opposite seasonal behavior. However both Cross-correlations indicate a negative correlation at around the 400-600 lag. As mentioned before when looking at figure A.1 on page 55, the climate volatility seems to be decreasing after 1.5 years, meaning around the 547 lag, which is exactly where the two Cross-correlations indicates a negative correlation relationship. Thus this confirms the lagged dependency property. It should be noted that as a result of the additional interpretation it is observed, that when the financial volatility spiked, indicating the markets worsens, the climate volatility diminished the years after, indicating the climate got better.

As mentioned before, the volatility spike in 2011 had a diminishing lagged effect on the climate volatility. However this raises the question of, what happening in that period. The article Elliott et al. [2011] explains, that August 8, 2011 the US and the global stock markets crashed due to a credit rating downgrade by the rating agency Standard & Poor's and as seen in figure A.7 on page 61 both financial measures are very much dependent on each other. This means, that this credit rating downgrade was responsible for the volatility spike of both markets in 2011, and therefore responsible for both markets crashing. Thus to summarize, the global stock market crash in 2011 lead to a decrease in the climate volatility in 2013. Furthermore the figures displaying Cross-correlation shows, that seasonal lagged dependency exist throughout the whole dataset, and thus also the 1.5 year negative correlation.

One of the aspects of interest was, if the difference in CO_2 emission had an observed effect on the climate volatility measure. However when looking at figure A.1 on page 55 and the figures of Cross-correlation no such correlation can be observed. In fact it seemed like the volatility of the countries of G7 had a even bigger effect on the climate volatility, when looking at the Cross-correlation coefficient values. This effect could be due to the two financial markets being too correlated.

However as mentioned before, when observing the Cross-correlations it seems that the CCF-SP-C reach higher absolute values than the CCF-BRIC-C. One implication not mentioned is that the climate volatility looks to have a larger impact on the volatility of S&P 500 index, than on the volatility of the MSCI BRIC index. When that is the case, this will result in the countries of G7 having a bigger initiative to stop climate change, since they will benefit more from it. This might also be one of the reasons for the BRIC countries releasing more and more CO_2 into the atmosphere.

Chapter 6

Conclusion

The purpose of this section is to discuss and conclude on the results presented in the previous chapters. We will discuss the results in the following section starting with a discussion of the different sections, conclusion of the results and lastly a perspectivation including ideas further research.

6.1 Discussion

This section introduces a discussion of the results of the thesis. The goal of this thesis is to analyse and construct volatility measures for climate and the financial market. Firstly a initial data analysis is conducted using the data from temperature anomalies, the S&P 500 index and the MSCI BRIC index. Then the data is filtered from deterministic seasonality in order to remove the seasonality effect. A time-varying parameter vector autoregressive model with stochastic volatility is then used in order to extract the volatility measures. Lastly the Cross-correlation is used in order to measure the correlation between the different volatility measures. The thesis will be discussed in the following small sections starting with the data analysis and ending with the model construction, which include the calculation of Cross-correlation.

6.1.1 Data Analysis

In chapter 4 on page 19, the data were introduced. Daily observations of temperature anomalies from 1880-2022 was used as a measurement of climate change. Using the information given by CO_2 emission, the financial data analysis was split into two regions, the G7 and the BRIC. Here it was assumed, that the S&P 500 index covers the financial market of the countries of G7. It was furthermore assumed, that the MSCI BRIC index covers the financial market of the countries of BRIC. Daily observations were obtained for both indexes, and then is was determined which time series to compare, and the length of the time series. Thus resulting in three groups labelled as C-SP, C-BRIC and C-SP-BRIC, with observations given in the period 2008-2022.

6.1.2 Deterministic Seasonality

In section 5.1 on page 28 some of the deterministic seasonality, such as yearly, half-yearly, etc. was filtered out to account for the existence of the deterministic seasonality. The seasonality function was determined using the p-values calculated from each parameter, and using the assumption of the existence of a linear dependence over time. The residuals were calculated, and labelled as Res-C-SP, Res-C-BRIC and Res-C-SP-BRIC.

6.1.3 Model Construction

Inspired by Alessandri and Mumtaz [2021] the vector autoregressive model with stochastic volatility were assumed for the data. This model was expanded by among others E. Primiceri [2005] and Nakajima [2011] into the time-varying parameter vector autoregressive model with stochastic volatility, which was used as a motivation to do the same. Here the Bayesian inference method was used with the Monte Carlo Markov Chain method, the Gibbs sampler. The Gibbs sampler was based on 50.000 iterations, where the first 5000 samples were discarded for convergence. Two years was used for calibration of the prior distribution, and the initial parameters was chosen as OLS point estimates. Number of lags were set to 1, where if a larger number of lags were used, the model might fit even better. Lastly scaling constants were introduced to the hyperparameters of the prior distribution.

The stochastic volatility of the TVP-VAR-SV models was extracted into the figures 5.2, 5.3 and 5.4 on respectively page 31, page 32 and page 33. A huge spike in the volatility for S&P 500 and MSCI BRIC was observed in the start of 2020, and it was assumed to be a result of the epidemic COVID-19. Therefore to try and get a more accurate volatility result, the TVP-VAR-SV models were also implemented in the period before COVID-19. Thus the figures 5.5, 5.6 and A.1 on respectively page 34, page 35 and page 55 were constructed, which used data from 2008-2020.

The most interesting result of the stochastic volatility was, that there seem to be a lagged dependency between the volatility of the S&P 500 index and the volatility of temperatures. Furthermore the lagged dependency could again be observed between the MSCI BRIC and temperatures. Here the Cross-correlation can be used in order to measure such dependency. Using the Cross-correlation with a radius set to 100 lags, it was observed, that there in fact seem to exist a lagged dependency property between the volatility measures in the period 2008-2022, where the volatility of temperatures after 25 days were correlated with the volatility of both the S&P 500 index and the MSCI BRIC index. Next the Cross-correlation was calculated in the period 2008-2020. This showed that the volatility of temperatures was correlated after several time stamps of both the S&P 500 and the MSCI BRIC index. This time the Cross-correlation was calculated with a radius of 700 lags in order to obtain the yearly effect.

The results from section 5.5 on page 36 and the results of section 5.3 on page 31 implicates a correlation between the climate volatility and the financial volatility. Combining the results confirms the lagged dependency between the volatility measures. This means, that using data from 2008-2022, the climate volatility gets diminished, when the financial volatility increases or spikes. However the further interpretation in section 5.6 on page 41 showed, that the difference in CO_2 emission between the countries of G7 and BRIC have no observed effect on the climate volatility measure. It should however be noted, that looking at the volatility measures and looking at the Cross-correlation figures showed clearly a lagged dependency between the financial volatility and the climate volatility. F.x. when the financial volatility spiked, indicating the markets worsens, the climate volatility diminished the years after, indicating the climate got better.

6.2 Conclusion

The problem statement is presented once more.

(i) **Analysis of climate- and financial volatility measures**

Which challenges arise, when constructing global volatility measures, and how is it possible to construct the volatility measures using techniques and methods from time series analysis?

(ii) **Dependence structure of these measures**

How can the dependence structure be measured? In recent years the countries of G7 has been focusing on reducing the CO_2 consumption, where the countries CO_2 emissions of BRIC, has been growing at a fast rate for more than a decade. Does this difference in CO_2 emission have an observed effect on the climate volatility measure? How is the volatility of the financial market dependent on the climate volatility?

(iii) **Reaction of these measures to climate disasters**

What is the connection between the climate volatility and the amount of climate disasters? Since the countries CO_2 emissions of BRIC is growing rapidly, this should be depicted in the climate volatility measure. How does the climate volatility and financial volatility react to this increased CO_2 emission?

Considering the discussion, the goal of analysing the climate- and financial volatility measures have been achieved by firstly obtaining the data, secondly using the deterministic seasonality function, and lastly constructing the time-varying parameter vector autoregressive model with stochastic volatility, thus constructing the volatility measures. The second goal of the project was to examine the dependence structure of these measures. This was done by inspection of the volatility measures observed in the sections 5.3 and 5.4 on respectively page 31 and page 34, and afterwards calculating the Cross-correlation observed in section 5.5 on page 36. The result was, that using data in the period 2008-2022, the climate volatility gets diminished, when the financial volatility increases or spikes, thus the volatility measures is correlated.

An interesting result was, that the difference in CO_2 emission between the countries of G7 and BRIC did not have an observed effect on the climate volatility measure. In fact it seemed like the volatility of the countries of G7 had a even bigger effect on the climate volatility, when looking at the Cross-correlation coefficient values. This is the result of the figures 5.7 and 5.9 respectively on page 5.7 and page 39. This effect could be due to the two financial markets being too correlated. However this effect means, that the countries of G7 does have a bigger initiative to stop climate change, since they benefit more from it. This could furthermore be one of the reasons for the BRIC countries releasing more and more CO_2 into the atmosphere.

In order to capture the reaction of these measures to climate disasters it was clearly seen, that when the epidemic COVID-19 started, the financial measure had a huge spike. Furthermore figure 5.4 on page 33 showed that the climate volatility decreased in the periods after. In order to capture the full effect, the model was constructed both in the period 2008-2022, and in the period before COVID-19 namely 2008-2020. The main difference was, that the full effect of the financial volatility could be observed, and to furthermore observed the effect of

the financial volatility spike on the climate volatility. The main result was, that looking at the volatility measures and looking at the Cross-correlation figures, they both showed a clear lagged correlation between the financial volatility and the climate volatility. The result of this observation was, that the climate volatility was decreasing in the years after a financial volatility spike, thus the climate get improved, when the financial markets worsen.

6.3 Perspectivation

This section introduces a perspectivation of the results of the thesis, including topics of further research.

In this thesis an time-varying parameter vector autoregressive model was used. The TVP-VAR-SV uses the notion of stochastic volatility inspired by Nakajima [2011] and E. Primiceri [2005]. As mentioned, this idea was proposed by Black [1976], which was followed by numerous developments in financial econometrics, f.x. the GARCH model, Heston model, etc. The GARCH models is, explained by Engle [2001,p. 157-168], used on data where the variances of the error terms may reasonable be expected to be larger for some points, i.e. the data are said to suffer from heteroskedasticity. This implementation could have proven to be an improvement on both the computational efficiency calculating the stochastic volatility, and might have been an improvement to the model. Furthermore the Heston model was proposed by Heston [1993,p. 327–343.] as an improvement to the Black and Scholes model. It describes the evolution of the volatility of an underlying asset, and it might especially have proven to be useful in calculating the volatility of the financial measures. Implementation of those models or others might lead to interesting results.

In this thesis the volatility measures are calculated using data from 2008-2022. However the dataset of the S&P 500 ranges all the way back to 1930. Furthermore the daily observations of temperature anomalies ranges all the way back to 1880. Thus using those dataset enables the possibility of modelling the climate volatility dependency on the volatility of the S&P 500 index from 1930 and forward. This could provide some interesting results. However due to the very large dataset, it could prove to be a computational difficult job for a computer. A solution could be to use other models, which might provide more computational efficient method. Furthermore the daily observations could be constructed to be monthly observations, which could improve the computational efficiency. A downside into using more data is that the S&P 500 were not traded as much in 1930, than it were traded in 2008

One of the main problems when testing if the difference in CO_2 emission have an observed effect on the climate volatility measure was, that the S&P index and the MSCI BRIC index might be too correlated. Thus for further research it could have been interesting to construct uncorrelated financial volatility measures of the countries representing respectively G7 and the BRIC, and see if those measures have an observed effect on the climate volatility measure.

Other ideas for further research:

- Construction of a better climate change measurement than temperature anomalies.

- Testing using the financial volatility of the entire worlds economic.

Bibliography

Alessandri and Mumtaz, **2021**. Piergiorgio Alessandri and Haroon Mumtaz. *The macroeconomic cost of climate volatility*, 2021. URL `https://arxiv.org/pdf/2108.01617.pdf?fbclid=IwAR20zL41eifLZHWbukN-eROQc18dDV6IfvukfJoH9KBfSPAZbnRR6rz2M2k`.

Bengtsson, **2021**. Henrik Bengtsson. *R.utils: Various Programming Utilities*. R package version 2.11.0, 2021.

Berkeley Earth, **2022**. Berkeley Earth. *Data Overview*, 2022. URL `http://berkeleyearth.org/data/`.

Black, **1976**. Fischer Black. *Studies of Stock Market Volatility Changes*. Proceedings of the American Statistical Association, 1976.

DataHub, **2022**. DataHub. *Standard and Poor's (S&P) 500 index Data including Dividend, Earnings and P/E Ratio*, 2022. URL `https://datahub.io/core/s-and-p-500`.

De Jong and Shephard, **1995**. Piet De Jong and Neil Shephard. *The simulation smoother for time series models*. Biometrika, 1995.

E. Primiceri, **2005**. Giorgio E. Primiceri. *Time Varying Structural Vector Autoregressions and Monetary Policy*. The Review of Economic Studies, 2005.

Eddelbuettel et al., **2022**. Dick Eddelbuettel, Romain Francois, JJ. Allaire, Kevin Ushey, Qiang Kou, Nathan Russell, Inaki Ucar, Douglas Bates and John. Chambers. *Rcpp: Seamless R and C++ Integration*. R packages version 1.0.8.3, 2022.

Elliott et al., **2011**. Larry Elliott, Jill Treanor and Dominic Rushe. *US credit rating downgraded to AA+ by Standard & Poor's*, 2011. URL `https://www.theguardian.com/business/2011/aug/05/ftse-slumps-us-jobs-data`.

Engle, **2001**. Robert Engle. *GARCH 101: The Use of ARCH/GARCH Models in Applied Econometrics*. Journal of Economic Perspectives, 2001.

Escribano et al., **2011**. Alvaro Escribano, J. Ignacio Peña and Pablo Villaplana. *Modelling Electricity Prices: International Evidence*. Oxford Bulletin of Economics and Statistics, 73,5 edition, 2011.

Explained, **2019**. Eurostat; Statistics Explained. *Glossary:Fossil Fuel*, 2019. URL `https://ec.europa.eu/eurostat/statistics-explained/index.php?title=Glossary:Fossil_fuel`.

finance, **2022**. Yahoo finance. *iShares MSCI BRIC ETF (BKF)*, 2022. URL `https://finance.yahoo.com/quote/BKF/history/`.

Geman and Geman, **1984**. Stuart Geman and Donald Geman. *Stochastic Relaxation, Gibbs Distributions, and the Bayesian Restoration of Images*. IEEE Transactions on Pattern Analysis and Machine Intelligence, 1984.

Gorjanc et al., **2022**. Gregor Gorjanc, Jana Obsteter and Thiago de Paula Oliveira. *AlphaPart: Partition/Decomposition of Breeding Values by Paths of Information.* R package version 0.9.1, 2022.

Hannah Ritchie and Rosado, **2020**. Max Roser Hannah Ritchie and Pablo Rosado. *CO2 and Greenhouse Gas Emissions.* Our World in Data, 2020. URL `https://ourworldindata.org/explorers/co2?facet=none&country=CHN~USA~IND~GBR~OWID_WRL&Gas=CO%E2%82%82&Accounting=Production-based&Fuel=Total&Count=Per+capita`.

Haugaard and Larsen, **2004**. Thomas Jensen Haugaard and Jens Anton Kjærgaard Larsen. *The BRIC Countries.* Monetary Review, 2004.

Heston, **1993**. Steven L. Heston. *A closed-form solution for options with stochastic volatility with applications to bond and currency options.* Review of financial studies 6.2, 1993.

Hoijtink, **2008**. Herbert Hoijtink. *Bayesian Data Analysis.* Department of Methodology and Statistics Utrecht University, third edition, 2008.

J. Keffer, **2015**. David J. Keffer. *A Practical Introduction to Applied Statistics for Materials Scientists and Engineers.* CreateSpace Independent Publishing Platform, first edition, 2015.

Judd, **1998**. Kennth L. Judd. *Numerical Methods in Economics.* Massachusetts Institute of Technology, 1998.

Kassambara, **2020**. Alboukadel Kassambara. *ggpubr: 'ggplot2' Based Publication Ready Plots.* R package version 0.4.0, 2020.

Kim and R. Nelson, **1999**. Chang-Jin Kim and Charles R. Nelson. *State-Space Models with Regime Switching.* The MIT Press, 1999.

Kim et al., **1998**. Sangjoon Kim, Neil Shephard and Siddhartha Chib. *Stochastic Volatility: Likelihood Inference and Comparison with ARCH models.* Review of Economic Studies, 1998.

Krueger, **2015**. Fabian Krueger. *bvarsv: Bayesian Analysis of a Vector Autoregressive Model with Stochastic Volatility and Time-Varying Parameters.* R packages version 1.1, 2015.

Laub, **2004**. Alan J. Laub. *Matrix Analysis for Scientists and Engineers.* SIAM: Society for Inductrial and Applied Mathematics, 2004.

Levy, **2012**. Roger Levy. *Probabilistic Models in the Study of Language.* University of California, San Diego, 2012.

Lynch, **2007**. Scott M. Lynch. *Introduction to Applied Bayesian Statistics and Estimation for social Scientists.* Springer, New York, NY, 1 edition, 2007.

Mahaboob et al., **2018**. B. Mahaboob, B. Venkateswarlu, C. Narayana, J. Ravi Sankar and P. Balasiddamuni. *A Treatise on Ordinary Least Squares Estimation of Parameters of Linear Model.* International Journal of Engineering & Technology, 2018.

Masnadi-Shirazi et al., **2019**. Hamed Masnadi-Shirazi, Alireza Masnadi-Shirazi and Mohammed-Amir Dastgheib. *A Step by Step Mathematical Derivation and Tutorial on Kalman Filters*. Other Statistics, 2019.

Metropolis et al., **1953**. Nicholas Metropolis, Arianna W. Rosenbluth, Marshall N. Rosenbluth, Augusta H. Teller and Edward Teller. *Equation of State Calculations by Fast computing Machines*. The Journal of Chemical Physics, 1953.

Mostafa and Mahmood, **2015**. Golam Mostafa and Monowar Mahmood. *The rise of the BRICS and their challenge to the G7*. International Journal of Emerging Markets, 2015.

MSCI, **2019**. MSCI. *The MSCI Principles of Sustainable Investing*. MSCI Inc, 2019.

Nakajima, **2011**. Jouchi Nakajima. *Time-Varying Parameter VAR model with Stochastic Volatility: An Overview of Methodology and Empirical Applications*. Monetary and Economic Studies, 2011.

Pörtner et al., **2022**. H.-O Pörtner, D.C. Roberts, M. Tignor, E.S. Poloczanska, K. Mintenbeck, A. Alegria, M. Craig, S. Langsdorf, S. Löschke, V Möller, A. Okem and B. Rama. *Climate Change 2022: Impacts, Adaptation and Vulnerability*. Contribution of Working Group 2 to the Sixth Assessment Report of the Intergovernmental Panel on Climate Change, 2022.

Rachev et al., **2008**. Svetlozar T. Rachev, John S. J. Hsu, Biliana S. Bagasheva and Frank J. Fabozzi. *Bayesian Methods in Finance*. John Wiley & Sons, Inc, second edition, 2008.

Robert and Casella, **2010**. Christian P. Robert and George Casella. *Introducing Monte Carlo Methods with R*. Springer, New York, NY, 1 edition, 2010.

Sedor, **2015**. Kelly Sedor. *The Law of Large Numbers and its Applications*, 2015. URL `https://www.lakeheadu.ca/sites/default/files/uploads/77/images/Sedor%20Kelly.pdf`.

Sharma, **2017**. Sanjib Sharma. *Markov Chain Monte Carlo Methods for Bayesian Data Analysis in Astronomy*. Annual Review of Astronomy and Astrophysics, 2017.

Slickcharts, **2022**. Slickcharts. *S&P 500 Companies by Weight*, 2022. URL `https://www.slickcharts.com/sp500`.

Smil, **2017**. Vaclav Smil. *Energy Transitions: Global and National Perspectives & BP Statistical Review of World Energy*, 2017. URL `https://ourworldindata.org/energy-production-consumption`.

Society, **2019**. National Geographic Society. *Fossil Fuels*, 2019. URL `https://www.nationalgeographic.org/encyclopedia/fossil-fuels/#:~:text=Fossil%20fuels%20are%20made%20from,are%20examples%20of%20fossil%20fuels.`

Spinu, **2021**. Vitalie Spinu. *lubridate: Make Dealing with Dates a Little Easier*. R package version 1.8.0, 2021.

Stephard and Harvey, **1989**. N. G. Stephard and A. C. Harvey. *On the probability of estimating a deterministic component in the local level model.* Journal of Time Series Analysis 11(4), pages 339–347, 1989.

Team, **2019**. R Core Team. *A Language and Environment for Statistical Computing.* R Foundation for Statistical Computing, Vienna, Austria, 2019.

Timothy and Joshua, **2004**. Derrick Timothy and Thomas Joshua. *Time Series Analysis: The Cross-Correlation Function.* Human Kinetics Publishers, 2004.

Vempala, **2005**. Santosh Vempala. *Geometric Random Walks: A Survey.* Combinatorial and Computational Geometry, 2005.

W. Nydick, **2012**. Steven W. Nydick. *The Wishart and Inverse Wishart distributions*, 2012. URL `https://swnydick.github.io/assets/reports/Wishart_Distribution.pdf`.

Wasserman, **2010**. Larry Wasserman. *All of Statistics: A Concise Course in Statistical Inference.* Springer, 2010.

Wickham, **2019**. Hadley Wickham. *ggplot2: Elegant Graphics for Data Analysis.* Springer-Verlag New York, 2019.

Wickham and RStudio, **2021**. Hadley Wickham and RStudio. *tidyverse: Easily Install and Load the 'Tidyverse'.* R packages version 1.3.1, 2021.

Wickham et al., **2019**. Hadley Wickham, Romain Francois, Lionel Henry and Kirill Müller. *dplyr: A Grammar of Data Manipulation.* R package version 0.8.3, 2019.

Wu et al., **2021**. Shu Wu, Majed Alharthi, Weihua Yin, Qaiser Abbas, Adnan Noor Shah, Saeed ur Rahman and Jamal Khan. *The Carbon-Neutral Energy Consumption and Emission Volatility: The Causality Analysis of ASEAN Region.* Energies, 14(10), 2021. ISSN 1996-1073. doi: 10.3390/en14102943. URL `https://www.mdpi.com/1996-1073/14/10/2943`.

Appendix A

Appendices

In this appendix, a few theoretical properties and some additional figures is presented, which is used in this thesis.

A.1 Miscellancous

This section is used to describe and present a few theoretical properties used in this thesis.

A.1.1 The Kronecker product

The Kronecker product possesses several properties, that often are used in order to solve difficult problems in linear algebra. It is an operation that transforms two matrices into a larger matrix, that contains all the possible products of the entries of the two matrices. The kronecker product is described by Laub [2004] in the following definition.

Definition 2: Kronecker products

Let $A \in \mathbb{R}^{m\times n}$, $B \in \mathbb{R}^{p\times q}$ be two matrices. Then the **Knonecker product** of A and B is defined as the matrix

$$A \otimes B = \begin{bmatrix} a_{11}B & \cdots & a_{1n}B \\ \vdots & \ddots & \vdots \\ a_{m1}B & \cdots & a_{mn}B \end{bmatrix} \in \mathbb{R}^{mp\times nq}$$

A.1.2 State space model

In this section, the State space model is presented. This is based on Kim and R. Nelson [1999].

Linear State-Space models are used in order to account for unobservable variables. The State-Space model consists of two equations: A State Equation and a Measurement Equation.

$$L_t = \theta L_{t-1} + \Upsilon l_t + W_t \qquad \textit{(The State Equation)}, \tag{A.1}$$

$$Y_t = AL_t + \Gamma l_t + V_t. \qquad \textit{(The Measurement Equation)}, \tag{A.2}$$

where

- L_t is a $n \times 1$ vector of unobserved state variables at time t,
- Y_t is a $k \times 1$ vector of observed measurement variables,
- A is a $k \times n$ matrix consisting of the relation between L_t and Y_t,
- θ is a $n \times n$ matrix consisting of the parameters of the time series model,
- l_t denotes a $r \times 1$ vector of inputs,
- Υ is a $n \times r$ matrix consisting of exogenous state variables,

- Γ is a $k \times r$ matrix consisting of exogenous measurement variables,
- $W_t \overset{iid}{\sim} \mathcal{N}_n(0, Q_{SS})$ is a $n \times 1$ White Noise vector,
- $V_t \overset{iid}{\sim} \mathcal{N}_k(0, R_{SS})$ is a $k \times 1$ White Noise vector.

The exogenous variables Υ and Γ can be set equal to the zero-matrix, if it is assumed that no exogenous variables are present. Furthermore W_t and V_t are the independent error terms.

The State equation (sometimes called the transition equation) is an unobserved equation that describes the dynamics of the state variables contained in L_t. However the Measurement equation describes the relation between the observed variables Y_t and the unobserved state variables L_t. The standard State-Space model is estimated using the *Kalman filter*.

A.1.3 Kalman Filter

This section is a continuation of the previous section. Thus it is based on Kim and R. Nelson [1999] as well.

The Kalman filter is a recursive procedure for computing the estimator of unobserved components, which in this case is the unobserved state variables $L_t = (L_1, \ldots, L_n)$. If the error term and the unobserved variables are normally distributed, the Kalman filter can calculate the likelihood function through the prediction error decomposition.

The estimates are obtained given data $\{Y_i\}_{i=1}^s$. It is called a filtering problem when $s = n$, thus the solution can be found using the Kalman Filter. The following notation is used throughout this section:

$$L_{t|s} = \mathbb{E}[L_t \mid \{Y_i\}_{i=1}^s]$$
$$P_{t|s} = \mathbb{E}[(L_t - L_{t|s})(L_t - L_{t|s})^T \mid |\{Y_i\}_{i=1}^s]$$

where $P_{t|s}$ is the conditional error covariance matrix.

The optimal estimate of L_t is obtained based on A_t, R_{SS} and Q_{SS} are known. The general idea of the Kalman filter is to specify the update from $L_{t|(t-1)}$ to $L_{t|t}$, once a new observation of Y_t is obtained, such that there is no need to process the entire dataset.

Proposition 1: Kalman Filter

Using the State-Space representation specified in equation A.1 on page 51 and equation A.2 on page 51 with initial conditions $L_{0|0} = \mu_0$ and $P_{0|0} = \Sigma_0$, the conditional expectation and conditional error covariance matrix can be written as:

$$L_{t|(t-1)} = \theta L_{(t-1)|(t-1)} + \Upsilon l_t,$$
$$P_{t|(t-1)} = \theta P_{(t-1)|(t-1)} \theta^T + Q_{SS}.$$

Now the Kalman filter updating algorithm can be specified as

$$L_{t|t} = L_{t|(t-1)} + K_t(Y_t - A_t L_{t|(t-1)} - \Gamma l_t),$$
$$P_{t|t} = (I_n - K_t A_t) P_{t|(t-1)},$$

where I_n denotes the identity matrix, and

$$K_t = P_{t|(t-1)}A_t^T(A_tP_{t|(t-1)}A_t^T + R_{SS})^{-1},$$

which is called the Kalman gain. Furthermore the Gaussian prediction errors can be calculated as

$$\begin{aligned}\varepsilon_{t,KF} &= Y_t - \mathbb{E}\left[Y_t \mid \{Y_i\}_{i=1}^{t-1}\right] \\ &= Y_t - A_tL_{t|(t-1)} - \Gamma l_t,\end{aligned}$$

and the corresponding covariance matrix is given by,

$$\begin{aligned}\Sigma_{\varepsilon_{t,KF}} = Var\left(\varepsilon_{t,KF}\right) &= Var\left(A_t(L_t - L_{t|(t-1)}) + V_t\right) \\ &= A_tP_{t|(t-1)}A_t^T + R_{SS}.\end{aligned}$$

Proof. For the proof see Masnadi-Shirazi et al. [2019,p. 24-25] □

A.1.4 The simulation smoother

This section is based on De Jong and Shephard [1995,p. 339-350] and Nakajima [2011].

The previous section described the Kalman filter, which could be used when $s = n$. However when $s > n$ the simulation smoother can be used. Thus conditional on all the parameters in the model $\omega = (\omega_0, \omega_1, \ldots, \omega_n)$, it is supposed that y_t is generated by the state space model (see section A.1.2 on page 51):

$$\begin{aligned}y_t &= X_t\beta + Z_t\alpha_t + G_tl_t, \quad t = 1, \ldots, n \\ \alpha_{t+1} &= W_t\beta + T_t\alpha_t + H_tl_t, \quad t = 0, 1, \ldots, n,\end{aligned} \tag{A.3}$$

where $\alpha_0 = 0$ and $H_tG_t^T = 0$. The u_t are independent $\mathcal{N}(0, I_n)$ variables, where the coefficients matrices may depend, implicitly, on ω_t.

Now the simulation smoother draws $\eta = (\eta_0, \ldots, \eta_t) \sim \pi(\eta \mid \omega, y)$, where $\eta_t = H_tu_t$, for $t = 0, \ldots, n$. Now the initial state is used, where $\alpha_1 = 0, P_1 = H_0H_0^T$, and therefore it is possible to recursively run the Kalman filter (see section A.1.3 on page 52):

$$\begin{aligned}\varepsilon_t &= y_t - X_t\beta - Z_t\alpha_t, & \alpha_{t+1} &= T_t\alpha_t + K_t\varepsilon_t, & K_t &= T_tP_tZ_t^TD_t^{-1} \\ P_{t+1} &= T_tP_tL_t^T + H_tH_t^T, & L_t &= T_t - K_tZ_t, & D_t &= Z_tP_tZ_t^T + G_tG_t^T,\end{aligned}$$

for $t = 1, \ldots, n$. Then the simulation smoother runs for $t = n, n-1, \ldots, 1$, thus let the initial values $r_n = U_n = 0$ and $\Lambda_t = H_tH_t^T$ be defined. Then the simulation smoother is run by:

$$\begin{aligned}C_t &= \Lambda_t - \Lambda_tU_t\Lambda_t, & \epsilon_t &\sim \mathcal{N}(0, C_t), \\ U_{t-1} &= Z_t^TD_t^{-1}Z_t + L_t^TU_tL_t + V_t^TC_t^{-1}V_t, & r_{t-1} &= Z_t^TD_t^{-1}\varepsilon_t + L_t^Tr_t - V_t^TC_t^{-1}\epsilon_t, \\ V_t &= \Lambda_tU_tL_t, & \eta_t &= \Lambda_tr_t + \epsilon_t,\end{aligned}$$

This means, that for the initial state the draws is $\eta_0 = \Lambda_0r_0 + \epsilon_0$. Thus replacing H_tl_t by η_t, and then computing α_t in the state equation A.3

A.1.5 Gibbs sampling for state space models

This section uses and gives a briefly introduction in the usability of the Gibbs sampling method for state space models. This section is based on E. Primiceri [2005].

Firstly start by consider a state equation equation without exogeneous variables:

$$L_t = \theta L_{t-1} + W_t,$$

and the corresponding measurement equation

$$Y_t = AL_t + V_t$$

where

$$\begin{bmatrix} W_t \\ V_t \end{bmatrix} \sim iid.\, \mathcal{N}\left(\begin{bmatrix} 0 \\ 0 \end{bmatrix}, \begin{bmatrix} Q_{SS} & 0 \\ 0 & R_{SS} \end{bmatrix} \right).$$

Now let

$$\begin{aligned} L_{t|s} &= \mathbb{E}\left[L_t \mid Y^s, A^s, Q^s_{SS}, R_{SS} \right] \\ P_{t|s} &= Var\left(L_t \mid Y^s, A^s, Q^s_{SS}, R_{SS} \right). \end{aligned}$$

Now initializing the values $L_{0|0}$ and $P_{0|0}$, then the standard Kalman filter from section A.1.3 on page 52 is used to derive

$$\begin{aligned} L_{t|t-1} &= \theta L_{t-1|t-1} \\ P_{t|t-1} &= \theta P_{t-1|t-1}\theta^T + Q_{SS} \\ K_t &= P_{t|t-1}A_t^T \left(A_t P_{t|t-1} A_t^T + R_{SS} \right)^{-1} \\ L_{t|t} &= L_{t|t-1} + K_t \left(Y_t - A_t L_{t|t-1} \right) \\ P_{t|t} &= P_{t|t-1} - K_t A_t P_{t|t-1} \end{aligned}$$

Now that the filtering is done, the last elements of the recursion are the mean $L_{n|n}$ and the variance $P_{n|n}$ of the normal distribution, which was used in order to make a draw for L_n. The draw of L_n and the output of the Kalman filter are now used for the first step of what is called the backward recursion. This will provide $L_{n-1|n}$ and $P_{n-1|n}$, which can be used to draw L_{n-1}. The backward recursion does the opposite of the *forward* recursion, and continues until time is zero. For a generic time t, the updating formulas of the backward recursion are:

$$\begin{aligned} L_{t|t+1} &= L_{t|} + P_{t|t}\theta^T P^{-1}_{t+1|t} \left(L_{t+1} - \theta L_{t|t} \right) \\ P_{t|t+1} &= P_{t|t} - P_{t|t}\theta^T P^{-1}_{t+1|t} \theta P_{t|t} \end{aligned}$$

A.2 Additional Figures

This section is used to describe and present a few additional figures, which were not presented in this thesis due to relevance of figures, and the choice of direction of this thesis.

A.2.1 SV from Res-C-SP-BRIC in 2008-2020

Presented is the stochastic volatility obtained by implementing the TVP-VAR-SV model using the residuals Res-C-SP-BRIC in the period 2008-2020.

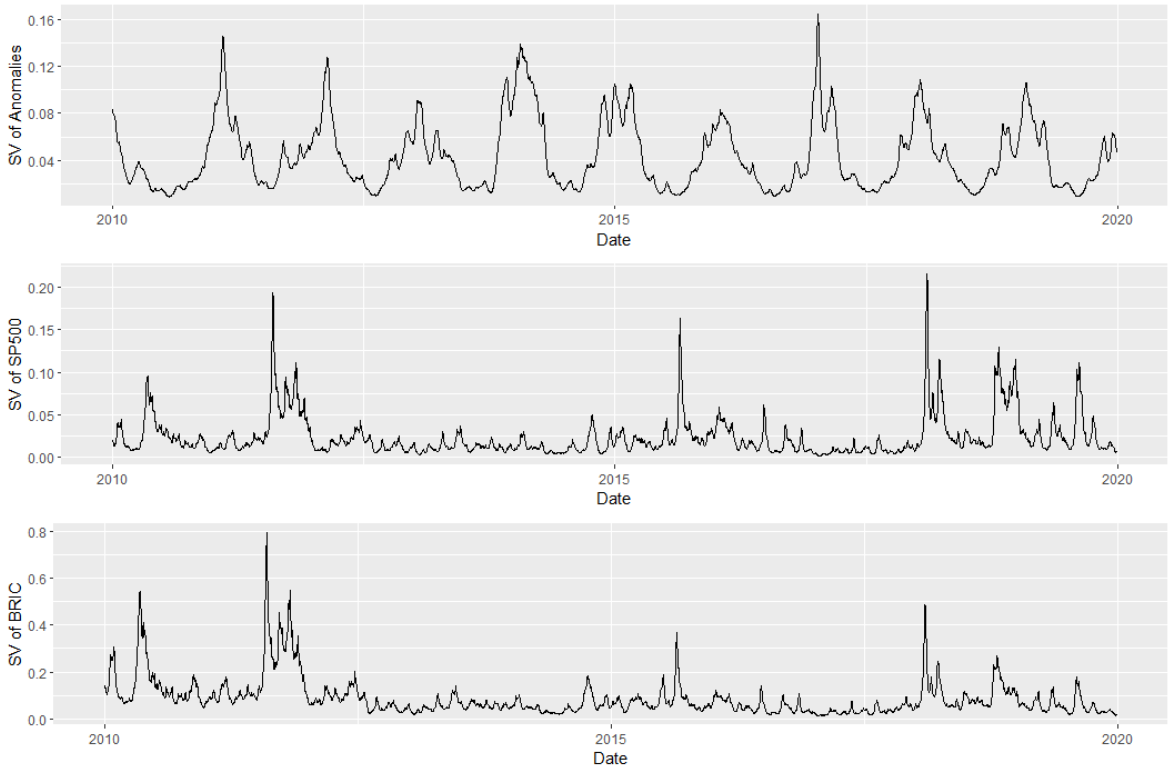

Figure A.1. Stochastic Volatility from TVP-VAR-SV using the comparison Res-C-SP-BRIC in the period 2008-2020.

A.2.2 Additional Cross-correlation plots

The CCF-SP-C and CCF-BRIC-C is calculated with the maximum values of T set to 700 using the data of Res-C-SP and Res-C-BRIC. The result is given in the following figures.

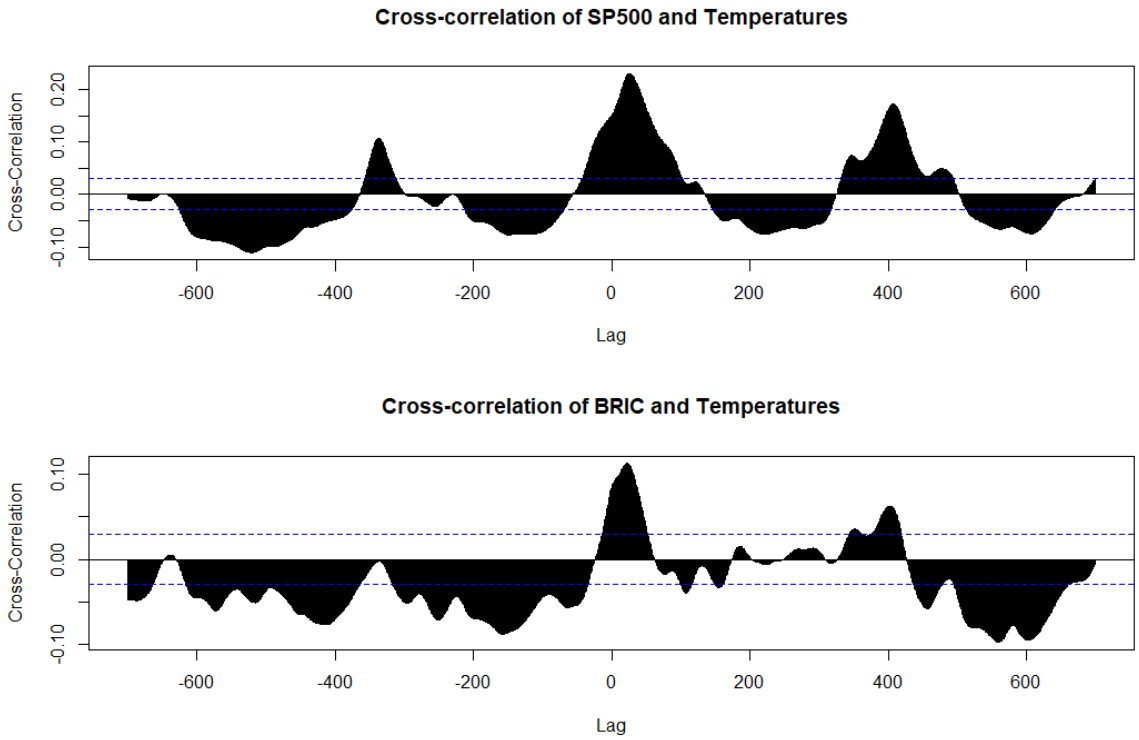

Figure A.2. Cross-correlation using the stochastic volatility of Res-C-SP and Res-C-BRIC with $max(|T|) = 700$.

The CCF-SP-C and the CCF-BRIC-C is calculated with the maximum values of T set to 700 using the data of Res-C-SP-BRIC. The result is given in the following figures.

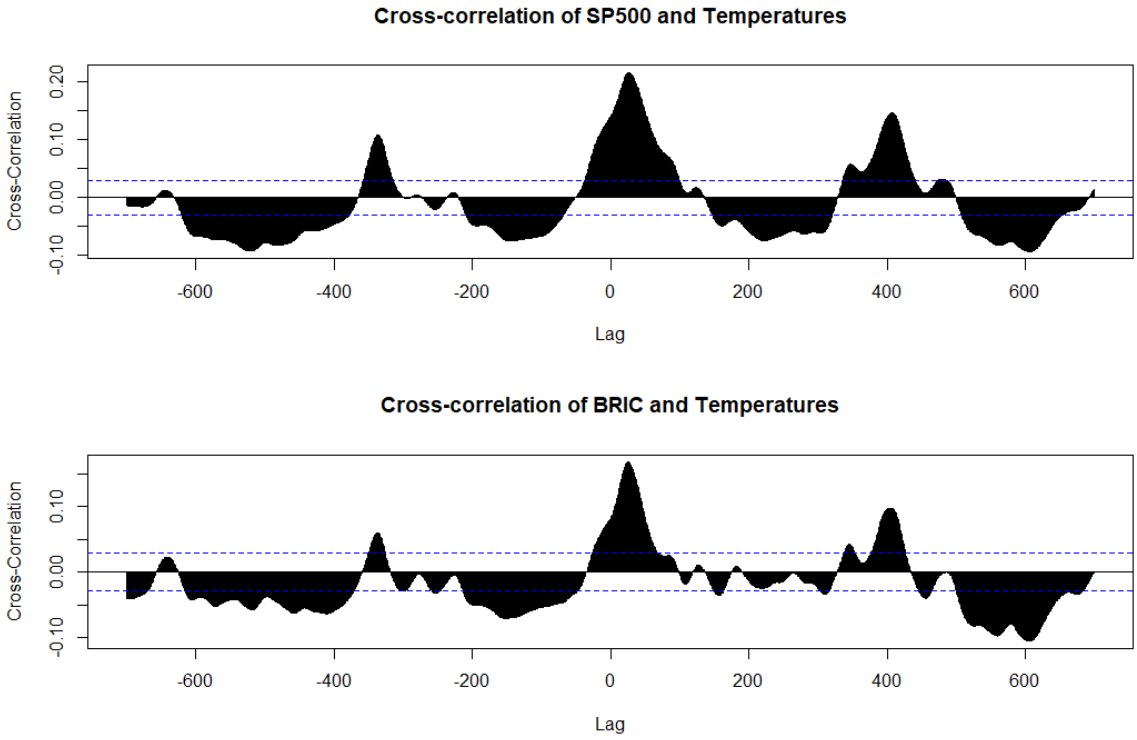

Figure A.3. Cross-correlation using the stochastic volatility of Res-C-SP-BRIC with $max(|T|) = 700$.

The CCF-SP-C and CCF-BRIC-C is calculated with the maximum values of T set to 100 using the data of Res-C-SP and Res-C-BRIC from 2008-2020. The result is given in the following figures.

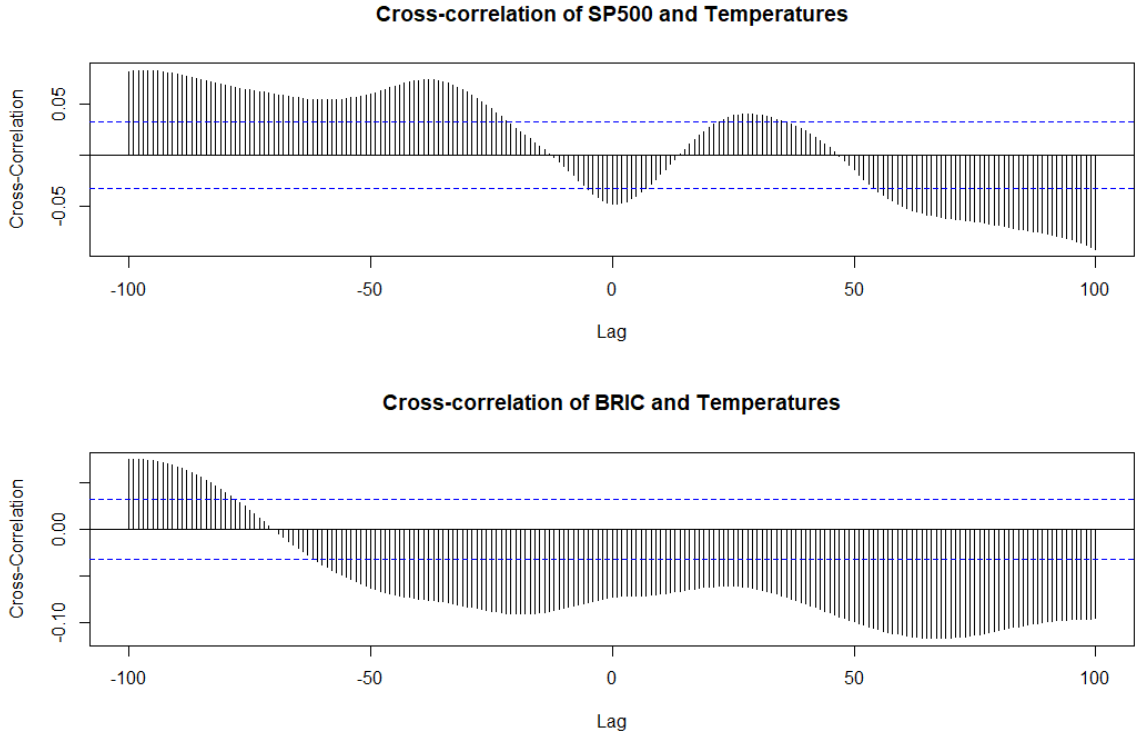

Figure A.4. Cross-correlation using the stochastic volatility of Res-C-SP and Res-C-BRIC from 2008-2020 with $max(|T|) = 100$.

The CCF-SP-C and CCF-BRIC-C is calculated with the maximum values of T set to 100 using the data of Res-C-SP-BRIC from 2008-2020. The result is given in the following figures.

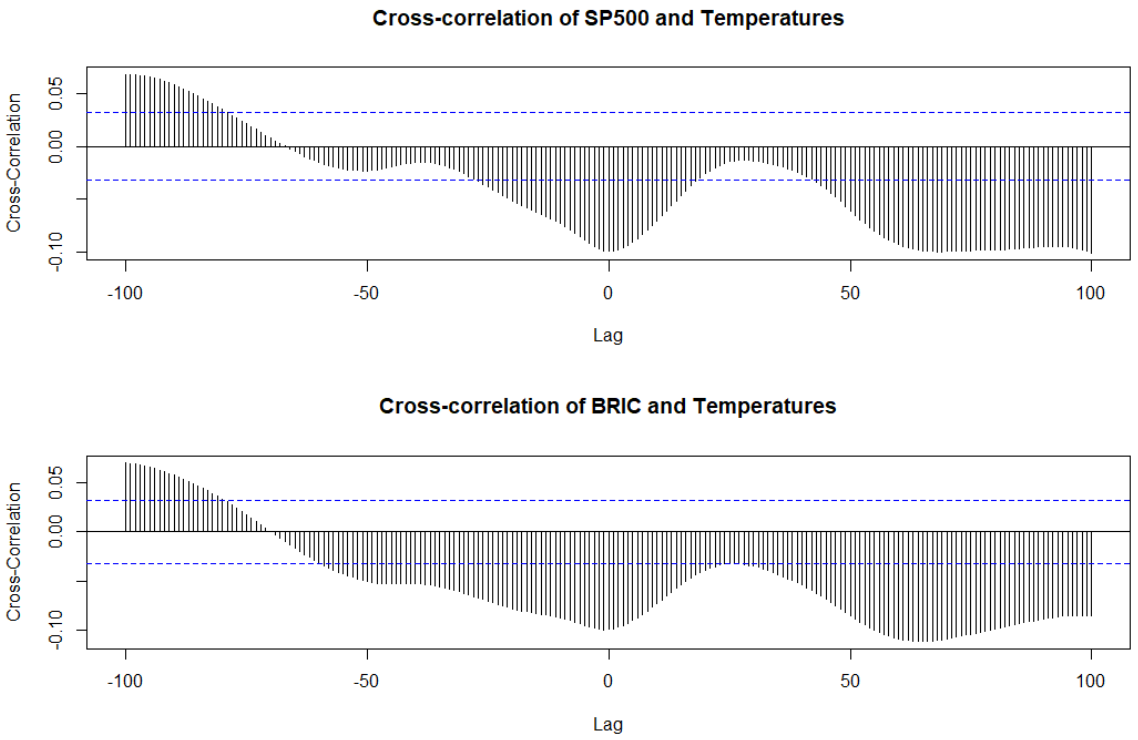

Figure A.5. Cross-correlation using the stochastic volatility of Res-C-SP-BRIC from 2008-2020 with $max(|T|) = 100$.

A.2.3 Cross-correlation between S&P 500 and BRIC

The Cross-correlation is calculated between the volatility of S&P 500 and the volatility of MSCI BRIC with the maximum values of T set to respectively 100 and 700 using the data of Res-C-SP-BRIC. The result is given in the following figures.

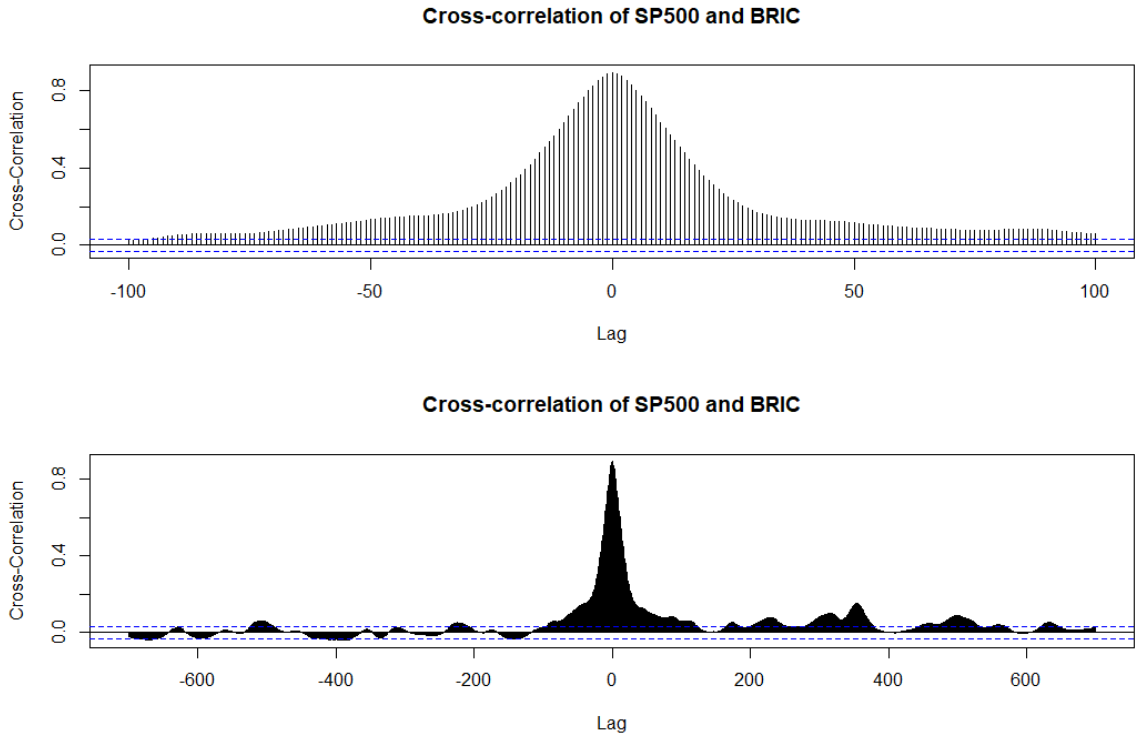

Figure A.6. Cross-correlation using the stochastic volatility of Res-C-SP-BRIC from 2008-2020 with $max(|T|) = 100$ and $max(|T|) = 700$.

The Cross-correlation is calculated between the volatility of S&P 500 and the volatility of MSCI BRIC with the maximum values of T set to respectively 100 and 700 using the data of Res-C-SP-BRIC in the period 2008-2020. The result is given in the following figures.

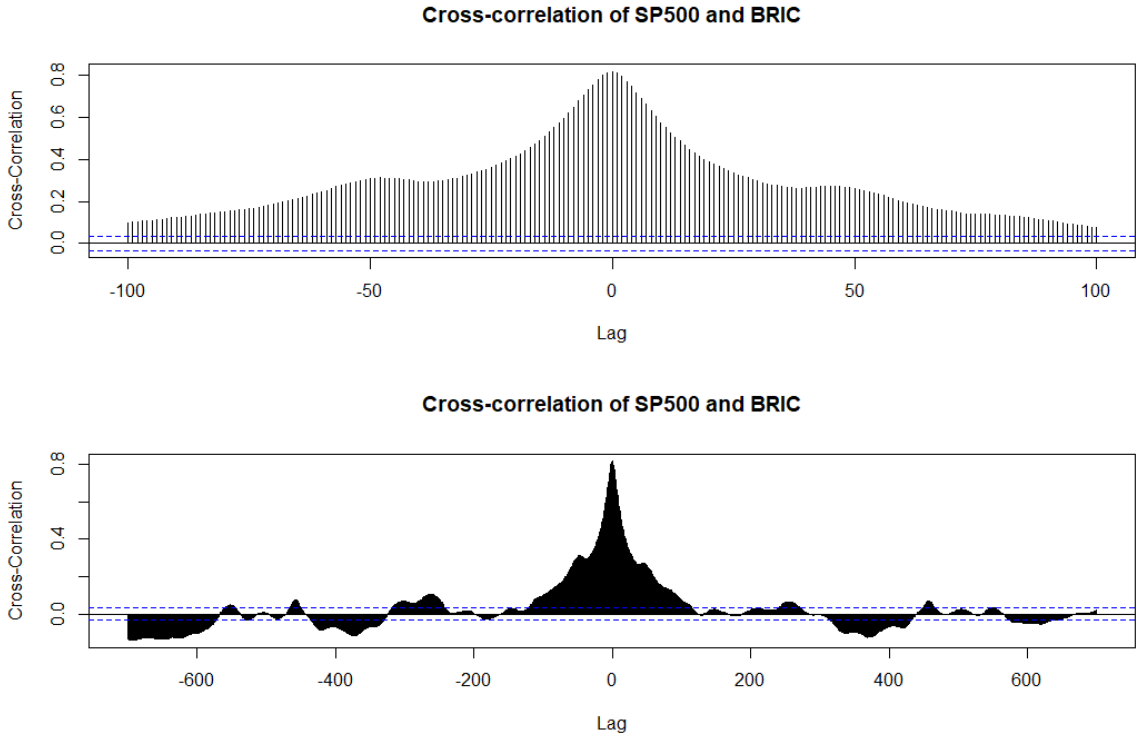

Figure A.7. Cross-correlation using the stochastic volatility of Res-C-SP-BRIC from 2008-2020 with $max(|T|) = 100$ and $max(|T|) = 700$.